Thermo-Mechanical Analysis of a Multi-Level Repository for Used Nuclear Fuel

NWMO TR-2012-19 **September 2012**

José L. Carvalho

Charles M. Steed

Golder Associates Ltd.
Golder Associates Report No. 11-1117-0045-TM-0002-00

NUCLEAR WASTE MANAGEMENT ORGANIZATION
SOCIÉTÉ DE GESTION DES DÉCHETS NUCLÉAIRES

Nuclear Waste Management Organization
22 St. Clair Avenue East, 6th Floor
Toronto, Ontario
M4T 2S3
Canada

Tel: 416-934-9814
Web: www.nwmo.ca

Thermo-Mechanical Analysis of a Multi-Level Repository for Used Nuclear Fuel

NWMO TR-2012-19

September 2012

José L. Carvalho
Charles M. Steed
Golder Associates Ltd.

ABSTRACT

Title: **Thermo-Mechanical Analysis of a Multi-Level Repository for Used Nuclear Fuel**
Report No.: **NWMO TR-2012-19**
Author(s): José L. Carvalho
Charles M. Steed
Company: Golder Associates Ltd.
Date: September 2012

Abstract

This report documents the thermo-mechanical analyses for the reference APM repository layout and addresses the optimization of the placement room spacing based on an alternate inventory of 7.2 million used CANDU fuel bundles placed in two repository levels. It also addresses the mechanical and thermally induced stress regimes and damage zones around the placement rooms and in-floor boreholes for the multi-level repository.

In addition to the impact of the containers on the in-floor boreholes and placement rooms (near field), the report addresses the thermally induced uplift at surface as well as any thermally induced distressed zone at surface (far-field) for the alternate inventory of 7.2 million used CANDU fuel bundles placed in two levels.

Through thermo-mechanical analysis of a unit cell of the repository (centreline to centreline of placement rooms, and centreline to centreline of containers), it has been established that, with the repository at depths of 400 m and 800 m with a fixed distance of 4.2 m between containers, the placement rooms can be spaced at 36 m centreline to centreline without the peak temperature of the containers exceeding 100°C. Alternatively, the placement rooms can be spaced at 32 m centreline to centreline in the upper level and 38 m centreline to centreline in the lower level without the peak temperature of the containers exceeding 100°C.

This optimised spacing of the placement rooms results in a footprint of 2 km × 1.45 km for both levels using the same spacing in both levels. Using the a different room to room spacing in each level, the footprint of the multiple level repository would be 2 km × 1.5 km for the lower level and 2 km × 1.3 km for the upper level.

Far-field analysis of the repository for the alternate inventory (7.2 million used CANDU fuel bundles) placed in two levels showed that the uplift over the centre of the repository is of the order of 40 cm and that the extent of the tensile zone is of about the same size as the footprint of the repository along the long and about double the width of the repository. The depth of the tensile zone at the time of its maximum extent (about 5000 years after placement) is of the order of 90 m.

TABLE OF CONTENTS

LIST OF TABLES

Page

LIST OF FIGURES

Page

1. INTRODUCTION

The Nuclear Waste Management Organization (NWMO) is implementing Adaptive Phased Management, Canada's plan for the long-term management of its used nuclear fuel (NWMO 2005, NRCan 2007). Adaptive Phased Management (APM) includes centralized containment and isolation of used fuel in a deep geological repository (DGR) in a suitable rock formation.

In 2011, the reference APM conceptual design and cost estimate was updated for a deep geological repository in crystalline rock for a base case inventory of 3.6 million used CANDU fuel bundles and an alternate case inventory of 7.2 million used CANDU fuel bundles. The fuel age is assumed to be 30 years out-of-reactor and the repository was assumed to be located on a single level at a depth of 500 m (SNC-Lavalin 2011).

In the conceptual design update of 2011, it was determined that the underground footprint of the repository for 3.6 million bundles was 1.5 km by 2.6 km (see Figure 1.1); this was based on a container centre-to-centre, in-floor spacing of 4.2 m and a placement room spacing of 40 m.

It was also recognized that there is room for design optimization of the APM repository layout and further analyses were undertaken to refine the room to room spacing (Carvalho and Steed, 2012). Another consideration for the repository layout is to determine the viability of a multi-level repository assuming an alternate used fuel inventory of 7.2 million used CANDU fuel bundles based on the following criteria:

- Alternate inventory of 7.2 million used CANDU fuel bundles;
- Used fuel containers are 30 years out-of-reactor at time of placement;
- In-floor placement method with a 10% borehole rejection rate;
- The repository levels should be located between 400 m and 800 m below ground surface;
- Used fuel placement commences in the lower repository;
- Used fuel placement in the upper repository starts 30 years after that of the lower repository;
- Interface between the used fuel container and the 30 cm thick bentonite buffer does not exceed 100°C for a multi-level repository; and
- The in-floor, centre-to-centre container spacing remains at 4.2 m.

This report documents the thermo-mechanical analyses for the multi-level APM repository layout and addresses the optimization of the underground footprint based on an alternate inventory of 7.2 million used CANDU fuel bundles, respecting the criteria presented above. It also addresses the mechanical and thermally induced stress regimes and damage zones around the placement rooms and in-floor boreholes for the multi-level repository assuming the geometry of the in-floor borehole and placement room as shown in Figures 1-2 and 1-3.

In addition to the impact of the containers on the in-floor boreholes and placement rooms (near field), the report will address the thermally induced uplift at surface as well as any thermally induced distressed zone at surface (far-field) for the alternate inventory of 7.2 million used CANDU fuel bundles.

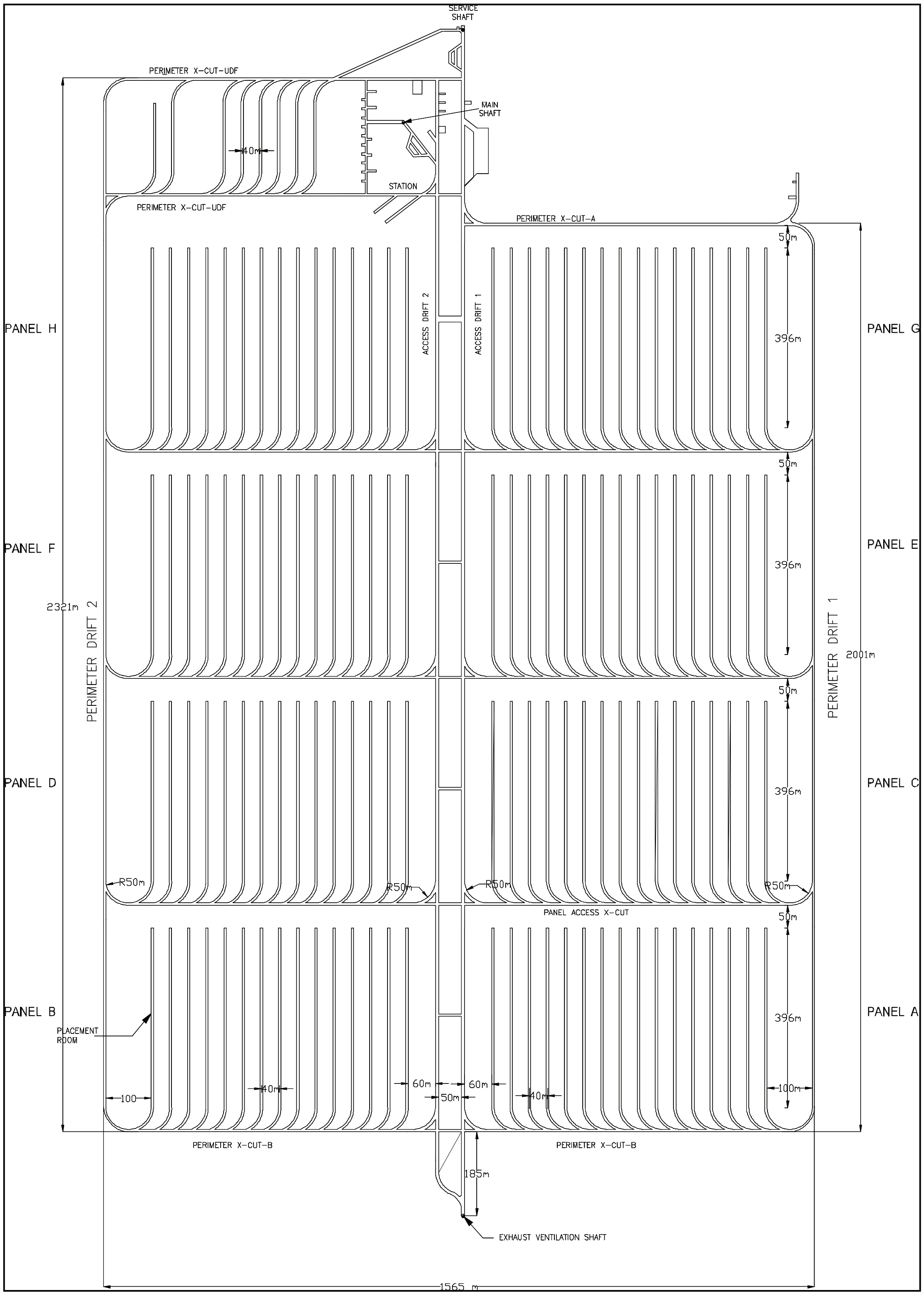

Figure 1-1: APM deep geological repository layout for 3.6 million used CANDU fuel bundles, including underground demonstration facility.

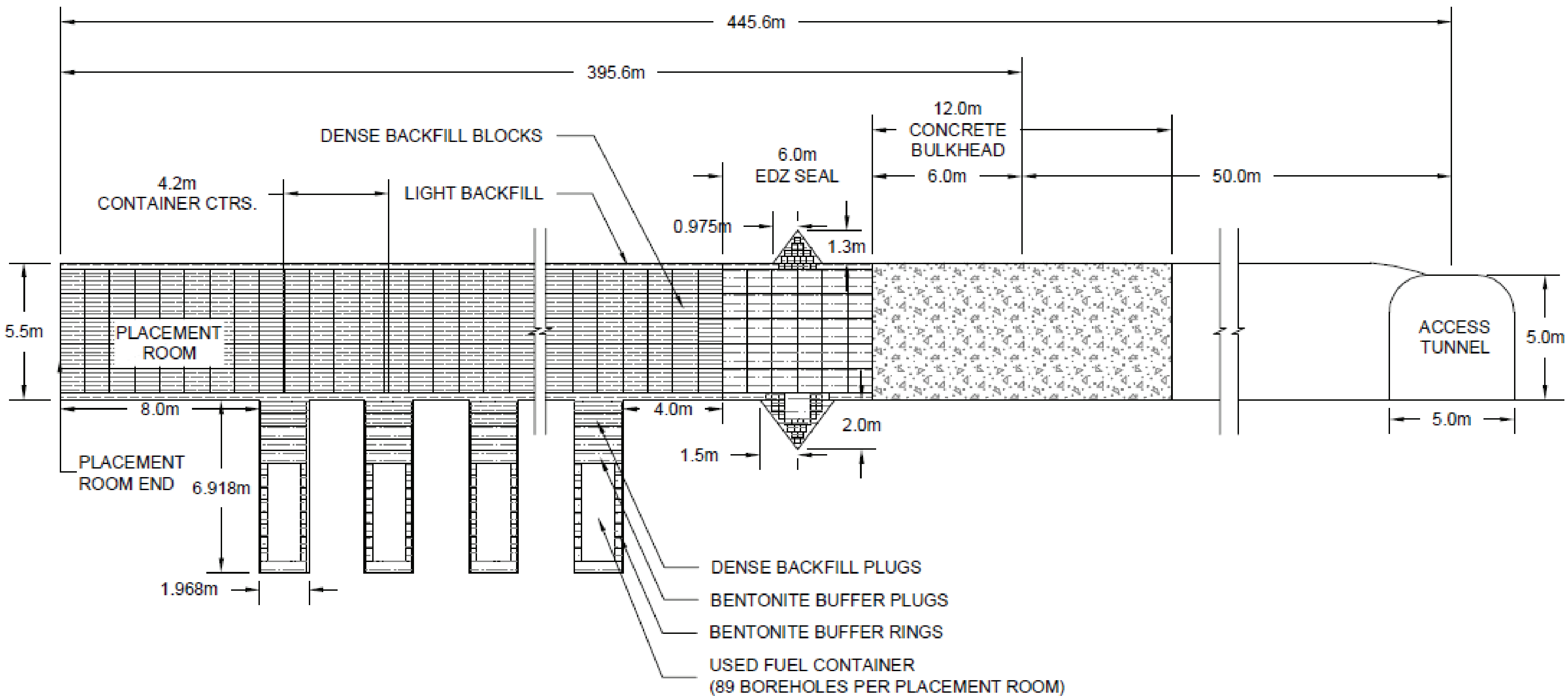

Figure 1-2: Section through APM placement room with in-floor borehole.

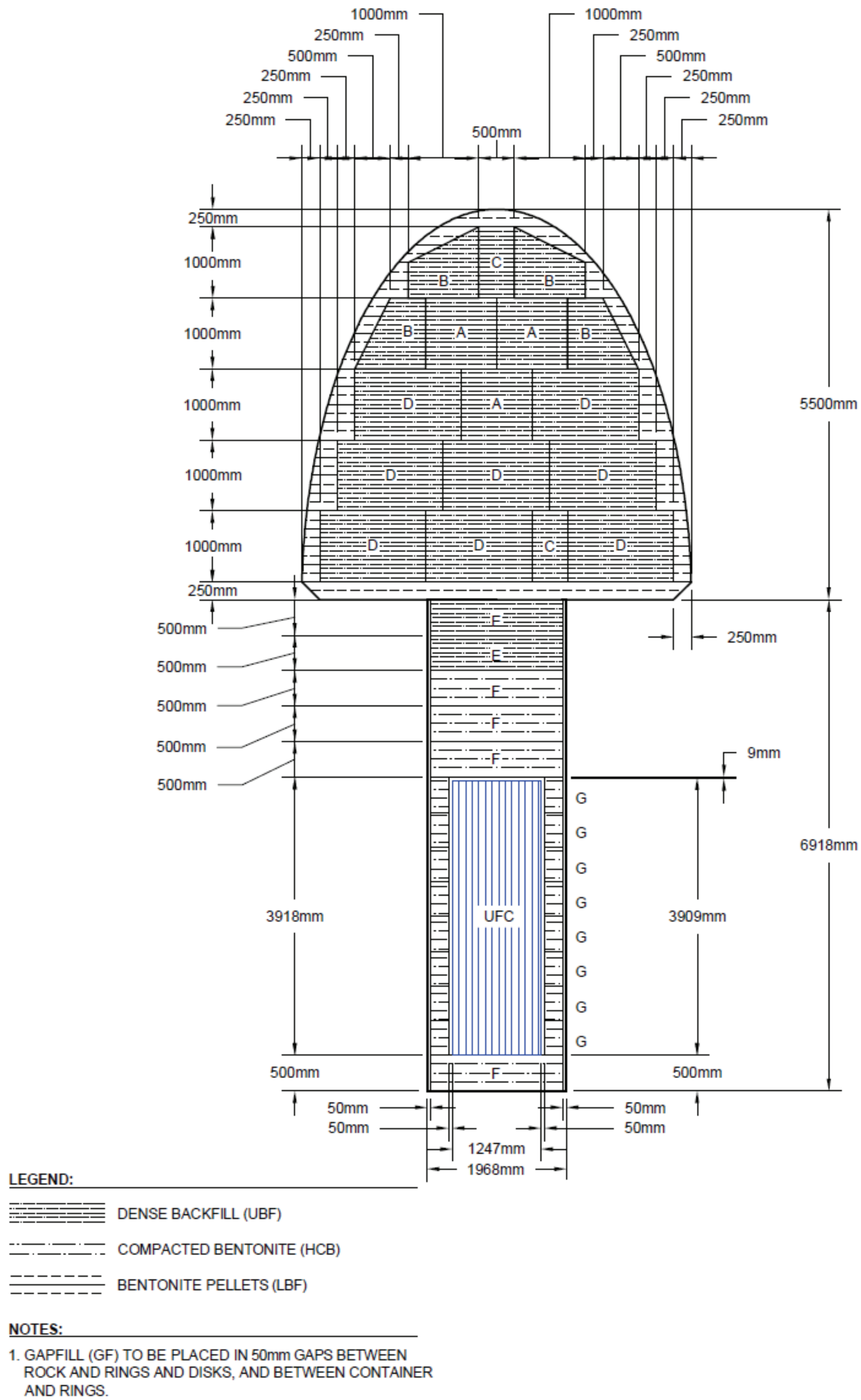

Figure 1-3: Cross-sectional view of APM placement room with in-floor borehole.

2. REPOSITORY GEOMEDIA DESCRIPTION

The reference crystalline geosphere is based upon the conditions encountered at the hypothetical geosphere defined for the Third Case Study (Gierszewski et al. 2004) and is assumed to be an elastic, isotropic, homogeneous, moderately to sparsely fractured granite (Garisto et al. 2004). The rock mass at the repository depth of 500 m would be defined as very good quality rock mass with an effective rock mass permeability of 10^{-15} m^2.

2.1 Geology

The Third Case Study developed a hypothetical site with characteristics and attributes that are similar to a typical Canadian Shield crystalline rock site.

2.2 Rock Types

In the reference crystalline geosphere one single rock type is considered, namely, granitic gneiss, which extends to surface.

2.3 Faulting

For the hypothetical Third Case Study site, a discrete fracture network was generated using a geostatistical fracture propagation procedure, the results of surface lineament analysis and lineament/fracture statistics for the Whiteshell Research Area (Srivastava 2002). Surface lineaments were extended into a self-consistent set of fractures to depths of 1500 m using propagation conditions that represent both sensible and geomechanically plausible fracture behaviour (Srivastava 2002).

An example of the model for a discrete fracture network over a hypothetical 84 km^2 region to a depth of 1500 m is shown in Figure 2-1 and the major fracture pattern at the 500 m repository level is shown in Figure 2-2.

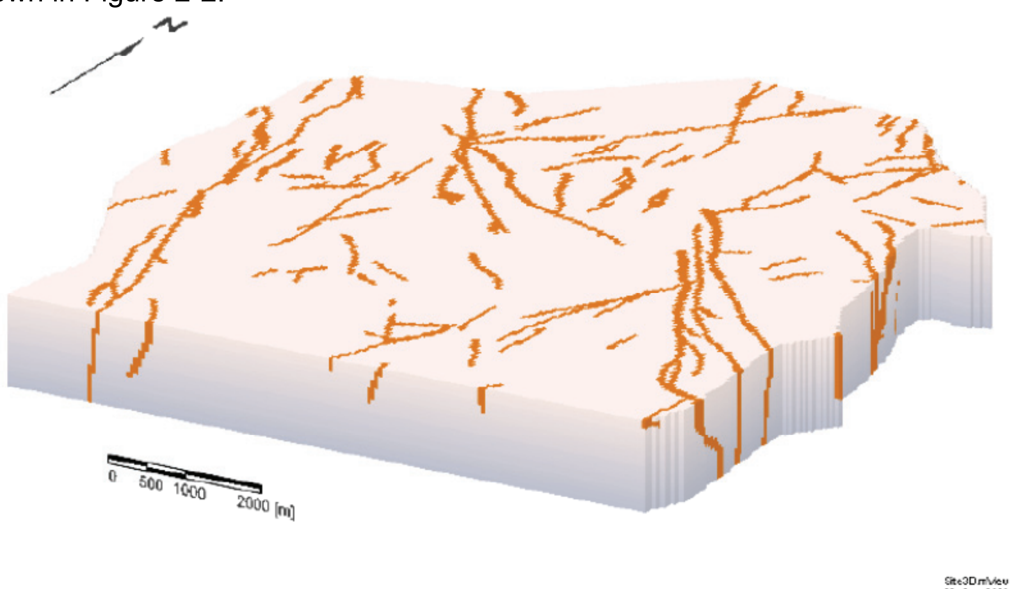

Figure 2-1: Reference Geosphere – Major faults and fractures between 500 m and 1500 depth.

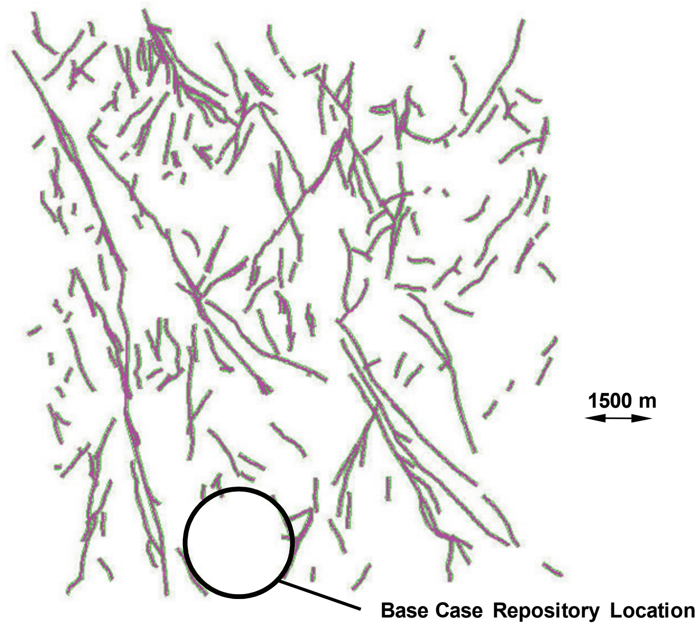

Figure 2-2: Reference Geosphere – Major Fracture Pattern at Repository Elevation (500 m depth).

For the hypothetical case it has been assumed that approximately 10% of the volume of the repository rooms excavated would not be useable for used fuel container (UFC) placement due to geotechnical or hydrogeological conditions.

3. GEOTECHNICAL AND GEOTHERMAL CHARACTERISTICS

The granitic gneiss (geomedia) was modelled using the Hoek-Brown criteria. Historically, two sets of strength parameters have been used to estimate the extent of damage around the rooms and the rock between the in-floor boreholes housing the containers. This is due to the fact that the analyses performed up to the 2011 update completed by SNC-Lavalin only considered linear elastic behaviour for the geomedia and as such, did not allow failure and re-distribution of stresses. Therefore, the stress field resulting from the excavation of the rooms was checked against one set of parameters and, if these were not exceeded, the stress field resulting from the heating process was checked against the second set of parameters (undamaged rock).

In the analyses conducted in the APM conceptual design update by SNC-Lavalin (2011) and for this report, the rock mass is modelled as an elasto-plastic material and the use of the two strength criteria as described above was not followed. Instead, the two criteria were adopted as the peak strength and the residual strength for the rock mass and the plastic algorithm in the numerical analyses handles the failure process and the change in rock mass strength internally. Density, elastic parameters, strength parameters and thermal properties for the granitic gneiss are presented below.

The backfill materials are not expected to experience stresses beyond their compacted strengths and as such they are modelled as elastic materials. Densities, elastic parameters and thermal properties for the backfill materials are presented below.

3.1 Rock Strength

The intact uniaxial compressive strength (UCS) for the granitic gneiss is specified as 210 MPa in the APM conceptual design update by SNC-Lavalin (2011) and in the design specifications. All other materials in the numerical model are modelled as elastic and do not require their strengths to be defined.

3.2 Rock Mass Quality

The rock mass quality for the crystalline rock was qualitatively described in the design specifications, which is consistent with that reported in the APM conceptual design update by SNC-Lavalin (2011). The given peak value of the parameter '*s*' in the generalized Hoek-Brown criterion, namely, *s* = 0.1, suggests a rock mass rating of RMR = 79 (equivalent Q = 50.4).

3.3 Rock Mass Strength Parameters for Numerical Analyses

Rock mass strength parameters are based on the UCS value given in the design specifications and reported by SNC-Lavalin (2011) combined with the estimation of rock mass quality in the previous section. It is assumed that the placement rooms will be excavated using careful blasting techniques, therefore no damage or negligible damage to the walls will result (D = 0).

The approach to rationalize the parameters for the modelling has been reported by SNC-Lavalin (2011) and suggests an intact value of m_i = 35, which is consistent with values for granite.

The residual parameters given in the design specifications suggest a drop in the value of RMR from 79 to 72 (peak to residual) representing the damage to the rock mass. It should be noted that at this range of rock quality, the Geological Strength Index (GSI) and the Rock Mass Rating (RMR) are interchangeable. The following parameters for peak and residual conditions were used in the analyses:

Peak:

$$s = e^{\frac{\mathrm{GSI}-100}{9}} = e^{\frac{79-100}{9}} = 0.1$$

$$m_b = m_i \times e^{\frac{\mathrm{GSI}-100}{28}} = 35 \times e^{\frac{79-100}{28}} = 16.5$$

$$a = \frac{1}{2} + \frac{1}{6}\left[e^{-\frac{\mathrm{GSI}}{15}} - e^{-\frac{20}{3}}\right] = \frac{1}{2} + \frac{1}{6}\left[e^{-\frac{79}{15}} - e^{-\frac{20}{3}}\right] = 0.501$$

$$\mathrm{UCS_{rm}} = s^a \times \mathrm{UCS_i} = 0.1^{0.501} \times 210 = 66.3\ \mathrm{MPa}$$

Residual:

$$s = e^{\frac{\mathrm{GSI}-100}{9}} = e^{\frac{72-100}{9}} = 0.0446$$

$$m_b = m_i \times e^{\frac{\mathrm{GSI}-100}{28}} = 35 \times e^{\frac{72-100}{28}} = 12.9$$

$$a = \frac{1}{2} + \frac{1}{6}\left[e^{-\frac{\mathrm{GSI}}{15}} - e^{-\frac{20}{3}}\right] = \frac{1}{2} + \frac{1}{6}\left[e^{-\frac{72}{15}} - e^{-\frac{20}{3}}\right] = 0.501$$

$$\mathrm{UCS_{rm}} = s^a \times \mathrm{UCS_i} = 0.0446^{0.501} \times 210 = 44.2\ \mathrm{MPa}$$

3.4 Rock Mass and Engineered Barrier Material Densities and Elastic Parameters for Numerical Analyses

The rock mass modulus given in the in the design specifications is 45 GPa. Using the value of RMR back-calculated in section 3.2, the elastic modulus of the intact rock would have been 51.6 GPa. This value for the intact modulus is slightly lower than expected for the reported strength of the granitic gneiss (UCS = 210 MPa), if the back-calculated value for RMR were to be assumed correct. Densities and elastic parameters for the rock mass and the engineered barrier materials are shown in Table 3-1.

Table 3-1: Mechanical Properties for the Rock Mass and the Engineered Barrier Materials

Material	Composition	Bulk Density (kg/m^3)	Dry Density (kg/m^3)	Young's Modulus (MPa)	Poisson's Ratio
Granitic Gneiss	N/A	2700	2700	45	0.25
Buffer - HCB	100% bentonite	1880	1610	0.10	0.10
Buffer Pellets - GF	100% bentonite	1439	1410	0.10	0.10
Dense Backfill - DBS	70:25:5 aggregate:clay:bentonite	2276	2120	0.20	0.10
Light Backfill - LBF	50:50 bentonite:crushed granite sand	1418	1240	0.10	0.10

3.5 Thermal Properties of Rock and Engineered Barrier Materials

The thermal properties for the geomedia and the backfill materials are given in the design specifications and shown in Table 3-2.

Table 3-2: Thermal Properties for the Rock Mass and the Engineered Barrier Materials used in the Analyses

Material	Composition	Thermal Conductivity (W/m°K)	Specific Heat (J/kg°K)	Linear Coefficient of Thermal Expansion (1/°K)
Granitic Gneiss	N/A	3.00	845	10^{-6}
Buffer - HCB	100% bentonite	1.00	1280	N/A
Buffer Pellets - GF	100% bentonite	0.40	870	N/A
Dense Backfill - DBS	70:25:5 aggregate:clay:bentonite	2.00	1060	N/A
Light Backfill - LBF	50:50 bentonite:crushed granite sand	0.70	1240	N/A

However, these differ somewhat from the thermal properties reported by SNC-Lavalin (2011) and shown in Table 3-3. It should be noted that, in the case of the in-floor method of placement in a crystalline rock mass, the thermal diffusion is dominated by the rock mass due to the proximity of the containers to the rock. This will be demonstrated later, where both sets of parameters were used for one of the trial layouts to quantify their impact on the results.

Table 3-3: Thermal Properties for the Engineered Barrier Materials reported by SNC-Lavalin (2011) – based on Baumgartner (2006) and Garisto et al. (2004)

Material	Composition	Thermal Conductivity (W/m°K)	Specific Heat (J/kg°K)	Linear Coefficient of Thermal Expansion (1/°K)
Buffer - HCB	100% bentonite	1.00	1440	N/A
Buffer Pellets - GF	100% bentonite	0.40	910	N/A
Dense Backfill - DBS	70:25:5 aggregate:clay:bentonite	2.00	1110	N/A
Light Backfill - LBF	50:50 bentonite:crushed granite sand	0.70	1280	N/A

4. IN SITU STRESS CHARACTERISTICS

In situ stress regimes for the crystalline geosphere were given in the design specifications and reported by SNC-Lavalin (2011) as:

From 0 m to 300 m:

$$\sigma_V = 0.0265 \times z;\ z \text{ in metres}$$

$$\sigma_H = 5.768 + 0.071 \times z;\ z \text{ in metres}$$

$$\sigma_h = 3.287 + 0.043 \times z;\ z \text{ in metres}$$

From 600 m to 1500 m:

$$\sigma_V = 0.0265 \times z;\ z \text{ in metres}$$

$$\sigma_H = 23.636 + 0.026 \times z;\ z \text{ in metres}$$

$$\sigma_h = 17.104 + 0.016 \times z;\ z \text{ in metres}$$

The in situ stress values between 300 m and 600 m should be linearly interpolated from the two stress regimes above. This results in the following relationships:

From 300 m to 600 m:

$$\sigma_V = 0.0265 \times z;\ z \text{ in metres}$$

$\sigma_H = 14.9 + 0.04056 \times z;\ z \text{ in metres}$

$\sigma_h = 5.67 + 0.035057 \times z;\ z \text{ in metres}$

It should be noted that the vertical stresses provided in the design specifications and reported by SNC-Lavalin (2011), were based on values provided by Kaiser and Maloney (2005), and do not match the vertical stress profile that results from the self-weight of the rock mass. Therefore, any model with a free surface will adjust the vertical stress to the self-weight of the material, regardless of its initial state. For this reason, the in situ vertical stresses were assumed to be gravitational, with a gradient matching the weight of the material.

5. GEOTHERMAL GRADIENT

The geothermal gradient has been defined as 0.012°C/m of depth with an average ground surface temperature of 5°C, resulting in an average rock and groundwater temperature of 9.8°C at a depth of 400 m and 14.6°C at a depth of 800 m.

6. THERMO-MECHANICAL NUMERICAL MODELLING

The numerical analyses undertaken in this study consist of thermo-mechanical coupled models both for the near-field and the far-field models. The software used in the analyses is FLAC3D v.4.00 Build 48-64 bit, which has been validated through a suite of runs against known solutions. FLAC3D is a finite difference code with capability to carry out coupled thermo-hydraulic-mechanic analyses.

6.1 Near-Field Modelling – Room Spacing Optimization

The numerical analyses undertaken for the near-field consist of a thermo-mechanical coupled model of a unit cell of the DGR. As such, the model is equivalent to two infinite repositories (400 m and 800 m deep) in which all containers are placed simultaneously in each repository; container placement takes place at the lower repository first, and container placement in the upper repository happens 30 years later. While this is not physically possible, it is a conservative model when trying to evaluate the temperature history of the near field up to about 500 years after UFC placement. The unit cell has a total height of 2000 m (the model mesh extends 1200 m below the lower repository horizon) and has a fixed lateral dimension of 2.1m (½ the container spacing). The other lateral dimension (½ the room spacing) was varied to determine the optimum spacing for the placement rooms and the repository levels, based on the criteria described in Section 1.

The placement method consists of an in-floor placement of the UFCs, in elliptically arched rooms of 5.5 m base and 5.5 m height. The containers are placed in 1.968 m diameter, 6.918 m deep boreholes drilled in the floor of the rooms. A 500 mm thick disk of highly compacted bentonite (HCB) buffer material is placed at the bottom of the hole, followed by 8 rings of the same material, totalling 3.918 m in height, and creating a cylindrical space for the container. Two gaps of 50 mm are left on both sides of the buffer rings; one annulus between the container and the inner side of the rings; the other annulus between the rock and the outer side of the rings. These gaps are filled with bentonite Gap Fill material. This assemblage is then topped by 3-500 mm disks of HCB buffer and 2 500 mm disks of dense backfill (DBF). The floor of the placement room is then levelled with 250 mm of light backfill (LBF) and blocks of dense backfill are placed to take up most of the room volume. After placement of the blocks of DBF, the space between the blocks and the rock are filled with LBF.

Figure 6-1 shows the FLAC3D mesh in an exploded view of the different components of the in-floor borehole and the placement room.

6.1.1 Mechanical Boundary Conditions

The vertical sides of the unit cell are prevented from moving (displacing) in the normal direction, generating symmetry conditions in both model faces of each horizontal direction. The top surface of the model is free to move in order to accommodate displacements caused by the excavation and the heating process. The lower boundary of the model is fixed in the vertical direction.

6.1.2 Thermal Boundary Conditions

An adiabatic condition (no heat flow) is imposed on the vertical sides of the model in order to respect the symmetry of the cells. The top surface of the model is kept at a temperature of 5°C, and a vertical temperature gradient of 0.012°C/m is applied to the model, resulting in a temperature of 29°C at the lower boundary of the model (2000 m below surface). The temperature at the lower boundary is fixed. These conditions are appropriate for the short-term near-field modelling conditions (i.e. approx. 500 years), which is well in advance of the onset of glaciations at which time the surface temperature is specified as dropping to 0°C. As the surface temperature cools, so will the temperature at the repository level, resulting in less severe thermal concentrations.

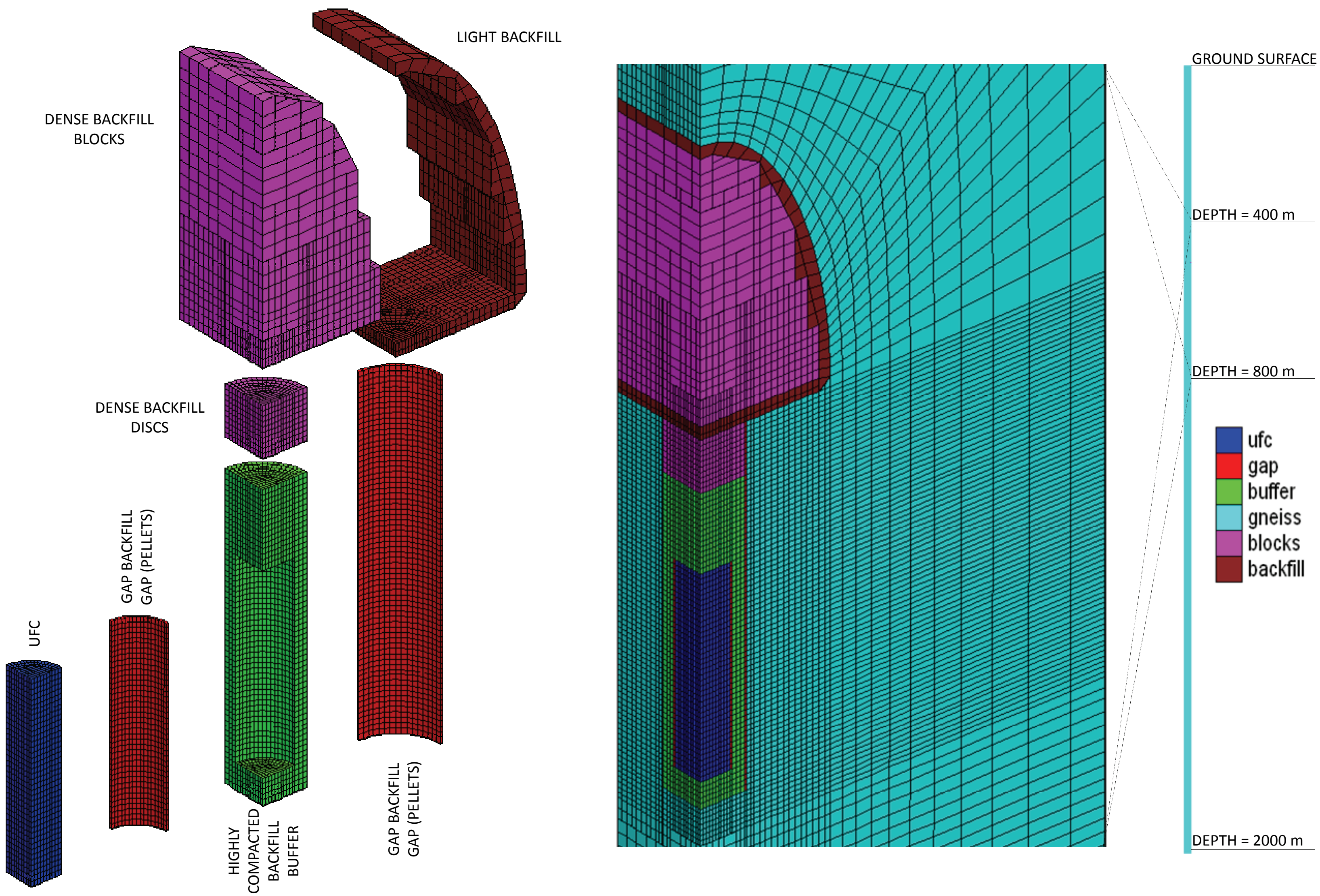

Figure 6-1: FLAC3D mesh for in-floor placement method – Crystalline geosphere.

6.1.3 Heat Generation

Heat is generated by the containers once they are placed in the repository. The following schedule for the IV 25 UFC heat output as specified in the design specifications was applied in the model:

Table 6-1: Used Fuel Bundle Heat Generation Rate at Various Times (Baumgartner 2006)

	Heat Generation (220 MWh/kg U Burn-up)		
Time Out-of-Reactor (years)	Watts per kg U	Watts per bundle	Watts per container (360 bundles)
30	1.83E-01	3.52	1268.2
35	1.68E-01	3.23	1164.2
40	1.54E-01	2.97	1069.2
45	1.42E-01	2.74	986.4
50	1.32E-01	2.53	910.8
55	1.22E-01	2.35	846.0
60	1.14E-01	2.19	788.4
70	9.91E-02	1.908	686.9
75	9.30E-02	1.791	644.8
80	8.75E-02	1.685	606.6
90	7.82E-02	1.505	541.8
100	7.07E-02	1.361	490.0
110	6.47E-02	1.245	448.2
135	5.41E-02	1.041	374.8
150	4.99E-02	0.96	345.6
160	4.77E-02	0.918	330.5
200	4.19E-02	0.806	290.2
300	3.55E-02	0.684	246.2
500	2.91E-02	0.56	201.6
1,000	2.02E-02	0.388	139.7
2,000	1.38E-02	0.265	95.40
5,000	1.00E-02	0.1926	69.34
10,000	7.19E-03	0.1385	49.86
20,000	4.16E-03	0.0801	28.84
35,000	2.27E-03	0.0437	15.73
50,000	1.43E-03	0.0274	9.864
100,000	4.41E-04	0.00849	3.056
200,000	1.65E-04	0.00317	1.141
250,000	1.52E-04	0.00293	1.055
500,000	1.48E-04	0.00285	1.026
1,000,000	1.48E-04	0.00285	1.026

The heat generation in the model is specified in W/m^3, therefore, a heat density generation is calculated by dividing the heat output of each container by the volume of the container. Heat generation was defined by the initial heat density, multiplied by a heat decay function (determined by normalizing the heat density generation, assuming 100% at 30 years out-of-reactor). The volume of the container (1.247 m dia. by 3.909 m high) is 4.774 m^3, resulting in an initial heat density generation of 265.644 W/m^3 at the time of placement (30 years out-of-reactor).

6.1.4 Thermal Results

The numerical analyses consisted of a thermo-mechanical coupled model and as such produced both temperature and stress/displacement results. However, the placement room spacing optimization is controlled exclusively by the temperature since the pillar width to room width ratio is large enough that the stresses around the rooms are not affected by their proximity and the distance between the repository levels are nearly two orders of magnitude larger than the room sizes.

The results from the single level repository indicate that the temperature history (timeline) exhibits two maxima (peaks); one at early time (between 15 to 40 years, depending on the placement room spacing), and a second one later on (between 1000 years and 3000 years, again, depending on the room spacing). Typically, for the single level repository, the temperature of the second peak does not exceed that of the first peak; however, in the case of the multi-level repository, it will be shown that the second peak (large time) will control the room spacing.

Based on these findings, the original models for the multi-level repository used the optimized room spacing for the single repository (i.e., 25 m centre to centre) as the starting point.

6.1.4.1 Thermal parameters reported by SNC-Lavalin (2011) vs design specification parameters

Two models with room spacing of 25 m and repository depths of 400 m and 800 m were run with two sets of thermal parameters for the engineered barrier materials, namely, those reported by SNC-Lavalin (2011) and those in the design specifications.

Figure 6-2 shows the time series for the lower and upper repositories using both sets of thermal properties. The results show that the difference in thermal properties of the engineered barrier materials has a very limited impact on the heat dissipation and the temperature history of the containers. This is attributed to the fact that the engineered barriers between the containers and the rock offer a small contribution to the resistance to heat flow due to their limited thickness (360 mm annulus).

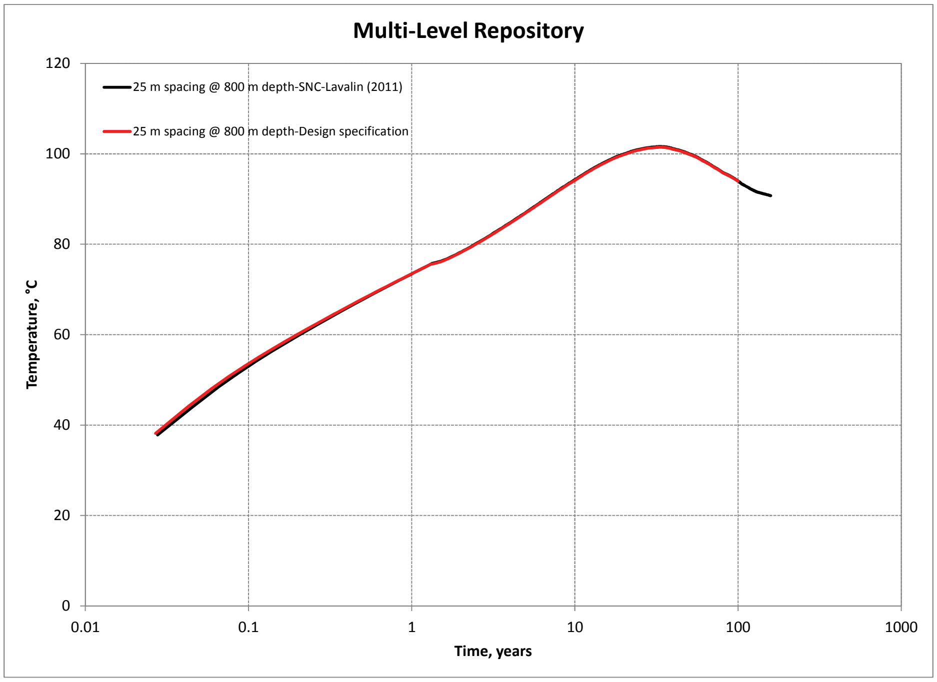

a) Temperature (°C) vs time (years) for the lower repository

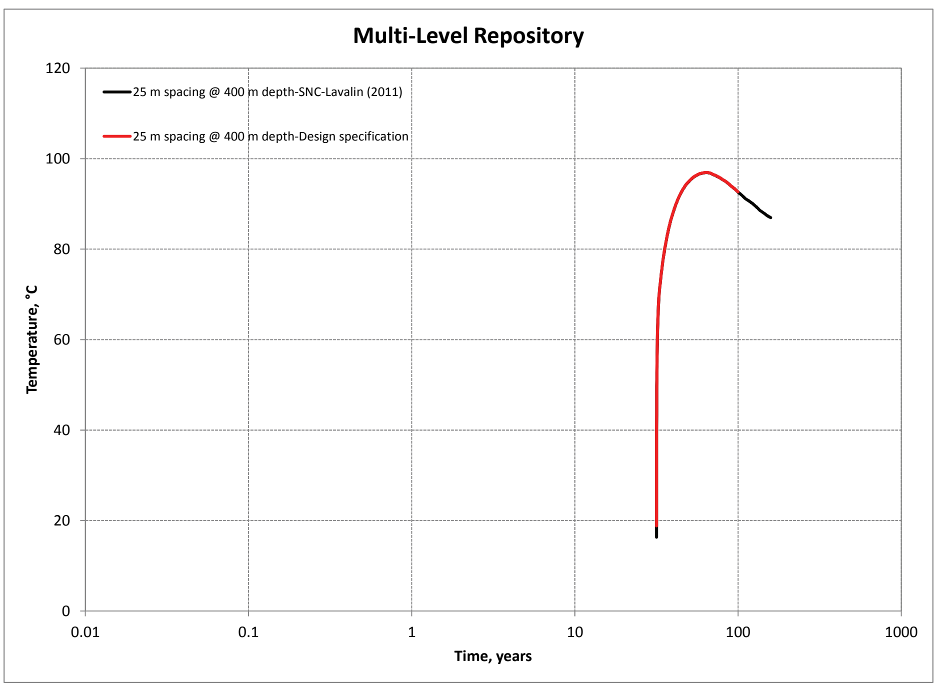

b) Temperature (°C) vs time (years) for the upper repository

Figure 6-2: Temperature time histories for results from two thermal parameter sets for the engineer barrier materials.

6.1.4.2 Effect of spacing between repository levels on early time response

One of the criteria for the multi-level repository requires that the two levels be located between 400 m and 800 m below ground surface. Therefore, two models, both with 25 m spacing between rooms, were set up to investigate the effect of the vertical proximity of the repositories. One model considered the repositories at the prescribed vertical limits, i.e., 400 m and 800 m depth; the other model considered half the vertical separation, i.e., repositories at 400 m and 600 m depth.

Figure 6-3 shows that the vertical separation between the repositories does not affect the early time response. The first temperature peak is a function of room spacing only; this is explained by the fact that the first temperature peak occurs long before one level feels the effect of the other level (typically in the 1000’s of years).

It should be noted that the maximum temperature reached in the lower repository at a depth of 800 m exceeds the 100°C by about 1.6°C, while the maximum temperature in the lower repository at a depth of 600 m reaches only 99°C. In both models, the upper repository reaches only 97°C. These differences in contrast with the single repository at a depth of 500 m can be attributed to the ambient temperatures at the repository depths, i.e., 9.8°C at 400 m, 11.0°C at 500 m, 12.2°C at 600 m, and 14.6°C at 800 m.

Also worthy of note is the time at which the temperature starts to rise for a second time. Both the time and the temperature of the second peak are controlled not only by the proximity of the placement rooms, but also by the vertical separation of the repository levels. Further discussion on the placement rooms and repository level spacing is presented in Section 6.1.4.4.

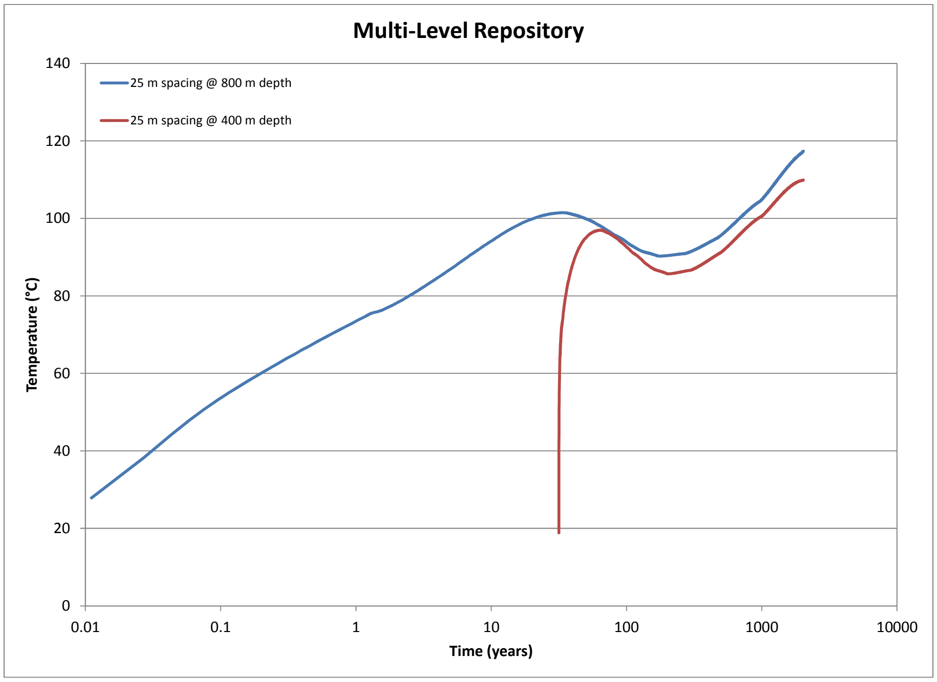

a) Temperature (°C) vs time (years) for a vertical separation of 400 m

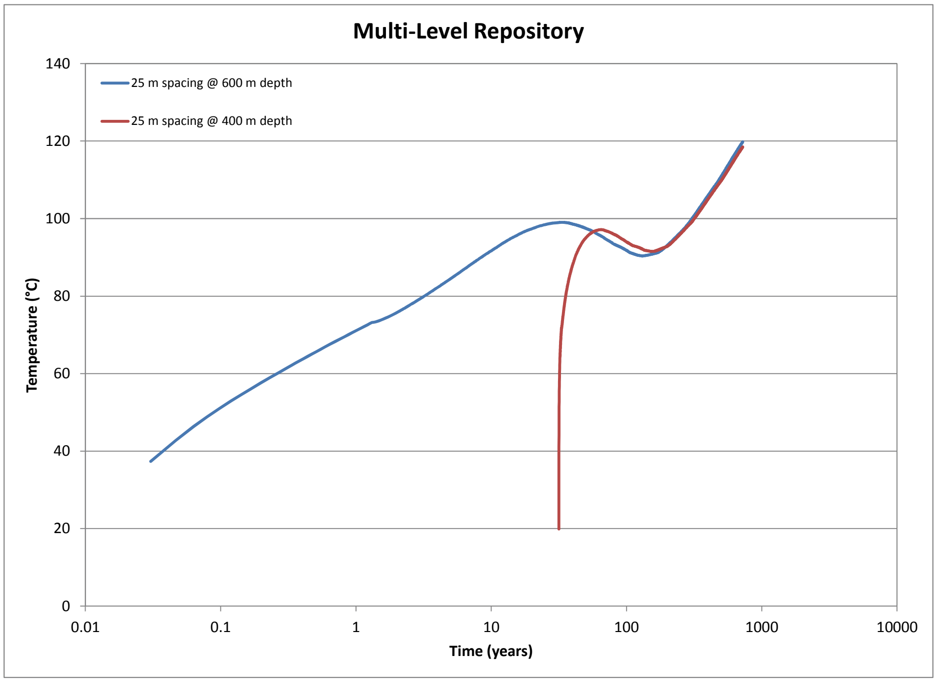

b) Temperature (°C) vs time (years) for a vertical separation of 200 m

Figure 6-3: Temperature time histories for results from two repository depths.

6.1.4.3 Comparison between results from a detailed mesh and a coarse mesh

While a detailed fine mesh (see Figure 6-1) allows for a very precise assessment of the temperature histories anywhere within the unit cell at early time, it has the drawback that the time step required for model convergence is too small to allow the assessment of thermo-mechanical behaviour at large times (> 1000 years). It has been observed from previous work on the single repository behaviour (Carvalho and Steed, 2012) that, at large times, the temperature of the unit cell becomes uniform because the rate of heat generation is of the same order of the rate of heat conduction across the cell.

Therefore, a coarse-mesh model with the ‘infinite’ repository heat density based on the unit cell was also analysed (height of cell assumed to be 5 m) for comparison to the near-field results and for the assessment of the large time temperature histories. In this case, the initial heat density generation of the repository layer (heat generation by unit volume) is given by:

$$\frac{1268.2\ W}{25\ \mathrm{m} \times 4.2\ \mathrm{m} \times 5\ \mathrm{m}} = 2.4156\ \mathrm{W/m^3}$$

Figure 6-4 shows temperature history locations for the fine-mesh analyses and Figure 6-5 shows the temperature timelines for those locations. In addition, the temperature timeline for cell in the coarse-mesh analysis is plotted in the same figure.

The comparison between the fine-mesh and coarse-mesh results allows for the following conclusions:

- The near-field temperature time history of the rock at the midpoint between the rooms (center of pillars) at the elevation of the container mid-height (purple line) is very closely replicated by the temperature time history at the centre of the coarse-mesh infinite repository (magenta dashed line).
- At the time of occurrence of the second peak, all tracked points at the container elevation in the near-field model are converging to a single temperature. The difference between the container temperature and the temperature at the midpoint between the rooms is less than 5°C.
- These findings are true for the repositories at both levels.
- The second temperature peak for the base case (room spacing of 25 m) grossly exceeds the target temperature of 100°C (135°C in the lower repository and 113°C in the upper repository).

The following effects of two geometric factors controlling the temperature of the repositories are worthy of note:

- A small increase in room spacing has a significant effect in the maximum temperature reached by the containers. The effect of changing the room spacing is a change in the effective heat conductivity for the ‘cell’ resulting in a faster dissipation of the heat.
- A multiple level repository (two levels) effectively impedes the ability for the repositories to dissipate heat in two directions (upwards and downwards) when compared to a single repository.
- The upper repository can dissipate heat faster than the lower repository because it has a more proximal boundary of constant temperature (ground surface at 5°C), as opposed to the lower repository, which escape route for the heat is towards a direction of continuously increasing in situ temperature (downwards).

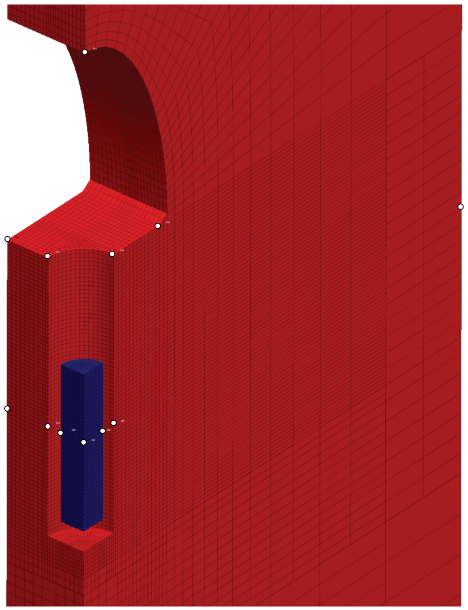

Lower Repository – 800 m below surface

Point	Location
216	Room Floor: r = 0.9835m - edge of hole perpendicular to drift
229	Room Floor: r = 2.5m - edge of room, perpendicular to drift
271	Room Floor: r = 0.9835m - edge of hole along drift
281	Room Floor: r=2.1m - along drift, C/L between containers
282	Container surface: r=0.6235m - between rooms
287	Rock surface: r=0.9835m - perpendicular to drift, between rooms
326	Rock: r=12.5m - C/L between rooms
327	Container centre
328	Container surface: r=0.6235m - along drift, between containers
333	Rock surface: r=0.9835m - along drift, between containers
343	Rock: r=2.1m - along drift, C/L between containers
344	Room Crown - above container

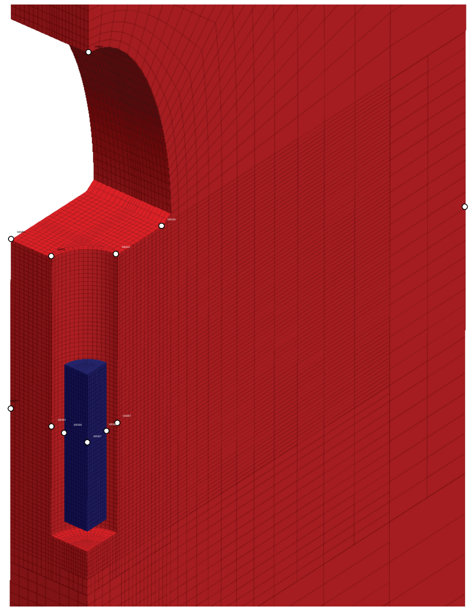

Upper Repository – 400 m below surface

Point	Location
100216	Room Floor: r = 0.9835m - edge of hole perpendicular to drift
100229	Room Floor: r = 2.5m - edge of room, perpendicular to drift
100271	Room Floor: r = 0.9835m - edge of hole along drift
100281	Room Floor: r=2.1m - along drift, C/L between containers
100282	Container surface: r=0.6235m - between rooms
100287	Rock surface: r=0.9835m - perpendicular to drift, between rooms
100326	Rock: r=12.5m - C/L between rooms
100327	Container centre
100328	Container surface: r=0.6235m - along drift, between containers
100333	Rock surface: r=0.9835m - along drift, between containers
100343	Rock: r=2.1m - along drift, C/L between containers
100344	Room Crown - above container

Figure 6-4: Temperature history locations.

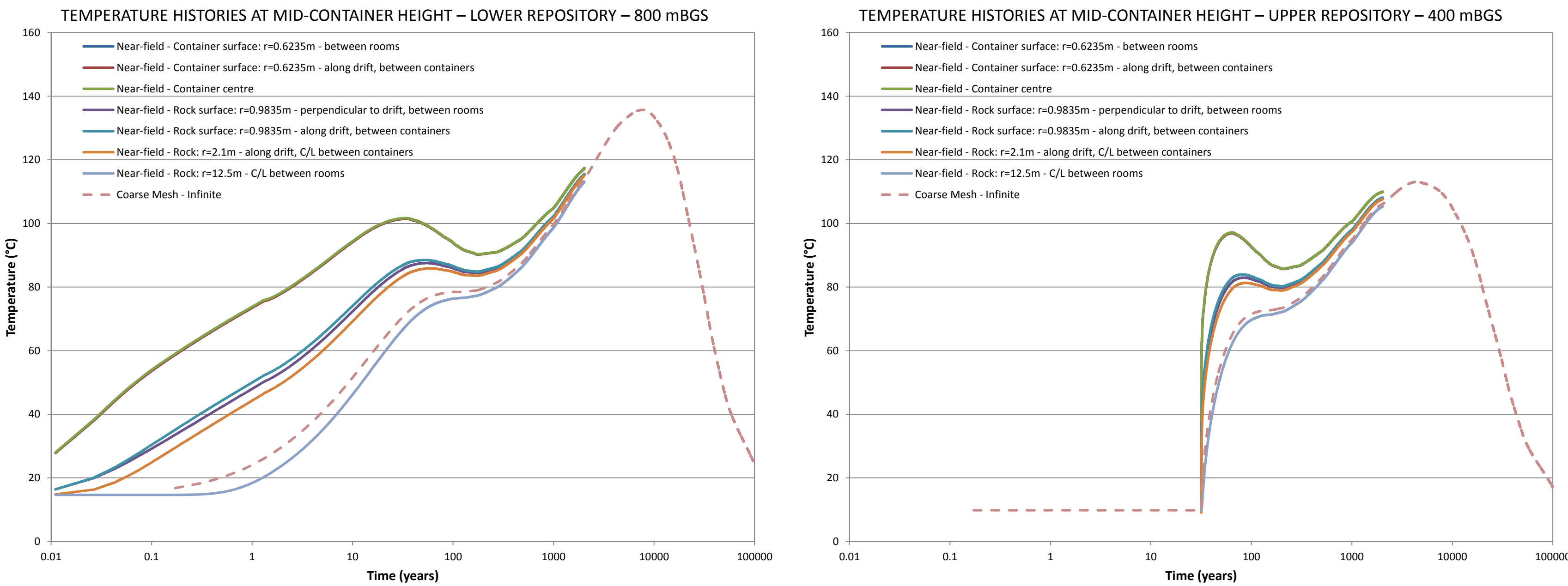

Figure 6-5: Temperature histories.

6.1.5 Optimization of room spacing

The results of the near-field analyses have demonstrated that, in the case of a multi-level repository, the second temperature peak controls the required spacing between the rooms. The analyses have also shown that, in order to minimize the room spacing, the vertical spacing needs to be maximized. Therefore, a number of models using the coarse mesh and designed to optimize the room spacing were set up for a multi-level repository with levels at 400 m and 800 m below ground surface.

Two arrangements were used to optimize the room spacing; the first adopted the premise that the room spacing should be the same in both repository levels; the second allowed for a different room spacing for each level to exploit the fact that the temperature in the upper level is considerably lower than that of the lower one and therefore, the rooms can be closer together. The following room spacing combinations were analysed to bracket the correct solution:

Same room spacing in both repository levels:

- 25 m spacing – room centre to room centre;
- 28.6 m spacing – room centre to room centre;
- 35 m spacing – room centre to room centre;
- 36 m spacing – room centre to room centre; and
- 37 m spacing – room centre to room centre.

Different room spacing in each repository level:

- 30 m spacing – room centre to room centre – in upper repository; 36 m spacing – room centre to room centre – in lower repository;
- 32 m spacing – room centre to room centre – in upper repository; 36 m spacing – room centre to room centre – in lower repository;
- 30 m spacing – room centre to room centre – in upper repository; 38 m spacing – room centre to room centre – in lower repository; and
- 32 m spacing – room centre to room centre – in upper repository; 38 m spacing – room centre to room centre – in lower repository;

The initial heat density of the repository layer (heat generation by unit volume) as a function of room spacing is given in Table 6-2.

Table 6-2: Initial Heat Density (W/m^3) as a Function of Room Spacing

Room Spacing (m)	Heat Generation (Watts per container)	Container Spacing (m)	Cell Height (m)	Initial Heat Density Generation (W/m^3)
25				2.4156
28.6				2.1116
30				2.0131
32	1268.2	4.2	5	1.8872
35				1.7254
36				1.6775
37				1.6322

38	1.5892

Figure 6-6 shows the temperature time histories for the several spacing combinations. The results for each run are colour coded with the solid lines representing the lower repository and the dashed lines representing the upper repositories.

Same room spacing in both repository levels:

The results show that the maximum temperature of the lower repository is under the target of 100°C for room spacings of 36 m or wider. Although the fine mesh analyses have shown that the container temperature can be a few degrees higher than the average cell temperature at the time of the second peak, this difference can be offset by the fact that the repositories are not ‘infinite’ (discussion on this in later) and also understanding that the containers are not all placed in the rooms at the same time.

Different room spacing in each repository level:

The results show that the maximum temperature of the lower repository is under the target of 100°C for all room spacings modelled (tightest spacing = 30m). In order to limit the temperature to 100°C in the lower repository, the room spacing will have to be 38 m or higher. It should be noted that the spacing of the rooms in the upper repository has a significant impact on the temperature of the lower repository, and consequently, in the required room to room spacing to meet the temperature criterion.

The following observations apply to both arrangements:

- The second temperature peak in the upper repository occurs 1200 to 1500 years earlier than that of the second repository, depending on the particular room arrangement.
- The second peak temperature of the upper repository is 10°C to 20°C cooler than that of the lower repository, depending on the particular room arrangement.

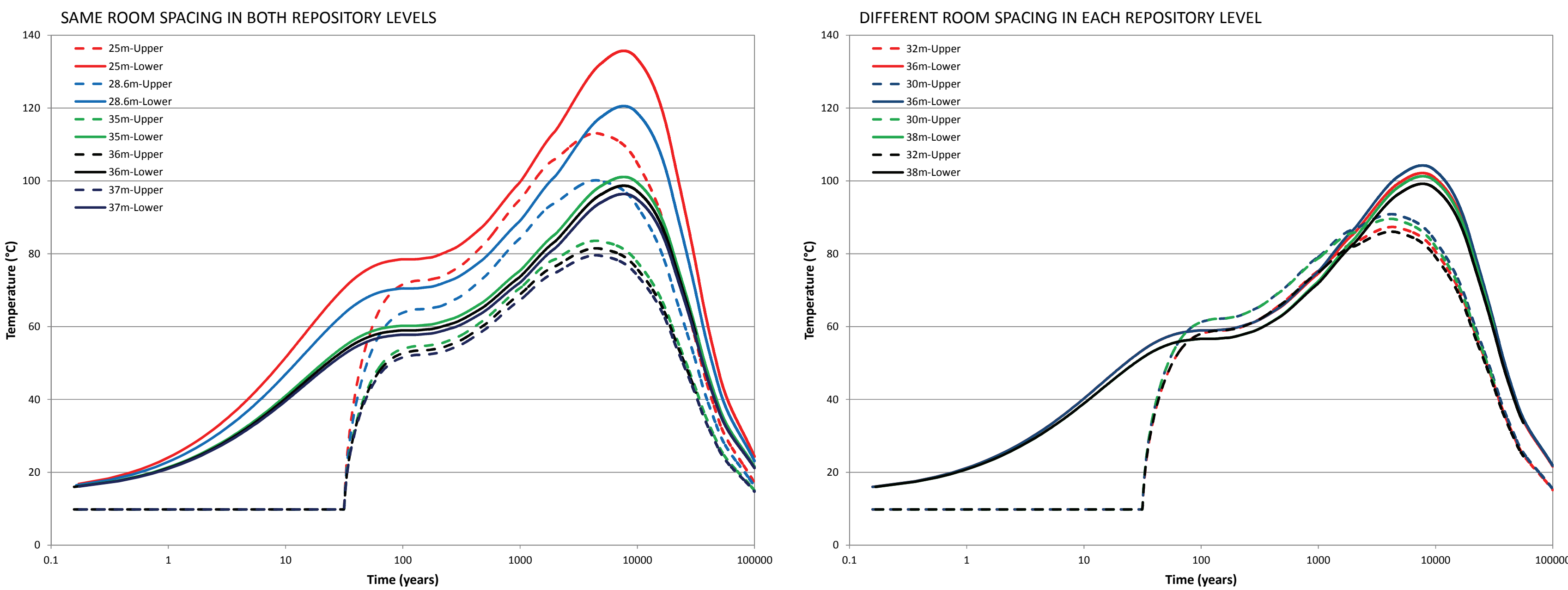

Figure 6-6: Temperature histories.

6.1.6 Room Stability and Rock Damage Extent for a 36 m Room Spacing Layout

Having set the placement room spacing at 36 m centre to centre, the assessment of the room stability and damage extent follows. Figure 6-4 shows the location of points at various distances from the container for which time histories were compiled, for a room to room spacing of 36 m (centreline to centreline), and an in-room container to container spacing of 4.2 m (centreline to centreline).

The lower repository is the more critical both from a mechanical and a thermal viewpoint. The in situ temperature and stresses are higher and the heat dissipation is not as efficient as in the upper repository. Therefore, the presentation of the results concentrates on the lower level. Figure 6-7 shows the time histories of temperature for the selected points for the lower repository shown in Figure 6-4. The temperature at the container walls peaks at a temperature of 88°C and 18.4 years after placement, while the rock in the walls of the borehole peaks at a temperature of 72°C and 36 years after placement.

Contours of temperature for different times after placement are shown in Figure 6-8. Although the blocks and the backfill in the rooms behave as insulators, slowing the vertical heat flow across the room, they have little impact on the temperature histories for the containers.

The major stresses around the placement room are shown in Figure 6-9 and are consistent with the rock damage shown in Figure 6-10. As the damage around the in-floor boreholes and the room floor deepens, the stresses are shed into the adjacent undamaged rock; this occurs right from the start of the excavation but it is much more evident in the later stages of heating, where damage is more extensive (around 36 years after placement).

Given the in situ stresses at the repository horizon, the uniaxial compressive strength of the granite and the rock mass quality estimation, the rock will experience minor damage in the first 10 cm or less around the excavations. The excavations are otherwise stable.

Figure 6-10 shows the evolution of the damage zone from the time of excavation of the room and placement of the containers to 100 years after placement. Damage from excavation is only surficial and is limited to 10 cm or less in the floor of the rooms. Heat from the containers induces thermal stresses and the damage zone extends to about 60 to 70 cm below the floor of the rooms along the centreline of the rooms (between containers). This depth of damage decreases from the centre of the rooms to the outer edges, where it is about 10 cm. The depth of damage at the centre of the rooms can in part be attributed to the flat floor. Negligible additional damage due to thermal stresses is shown on the sides and crown of the excavation.

The damage around the boreholes and rooms is further divided in to three zones. These zones are defined based on potential changes in flow and transport properties, and they are:

- The Excavation disturbed Zone (EdZ) – is a zone with hydromechanical and geomechanical modifications, without major changes in flow and transport properties.
- The Excavation Damage Zone (EDZ) – is a zone with hydromechanical and geomechanical modifications, including significant changes in flow and transport properties.
- The Highly Damaged Zone (HDZ) – is a zone where macro scale cracking or spalling may occur. The effective permeability of this zone is dominated by the interconnected fracture system and may be significantly greater that the matrix permeability.

Criteria to determine the boundaries between these zones need to be defined to make the process consistent and defensible. The minor plastic strain combined with the thresholds the crack initiation and crack damage, as defined in a uniaxial compression test, were used to estimate the extent of the damage zones. For strong brittle rocks like granite, which behave fairly linearly until failure, the total strain at failure can be estimated by the ratio of the peak strength to the elastic modulus. Using the parameters reported in Section 3.4, namely, UCS = 210 MPa and Ei = 51 GPa, the strain at failure is 0.0041. Typically, crack initiation starts at approximately 0.4 × UCS and crack damage occurs at approximately 0.7 × UCS; therefore, the threshold strain for the HDZ/EDZ boundary and the EDZ/EdZ boundary are 0.00288 and 0.00164, respectively.

Using these strain values, the extent of the HDZ and EDZ are shown in Figure 6-11 at a time of 30 years after placement (temperature first peak). Figures 6-11 a) and b) show the full range of total strain (elastic and plastic) and the range of total strain above the crack initiation limit. There is no distinguishable difference between the two figures, indicating that the strain contours in the figure represent the combined EDZ and HDZ extents. Figure 6-11 c) shows the extent of the full plastic zone (inclusive of all damage zones) marked as yielded or at yield; this zone has the same extent as in Figure 6-11 d), which shows the full range of the plastic strain. Finally, Figure 6-11 e) shows the HDZ (in red) and the EdZ (in blue), with the contours between those two zones representing the EDZ. Figure 6-11 e) indicates that the EDZ is very localized, representing a quick transition between the HDZ and the EdZ. This is typical of very strong brittle rocks which tend to exhibit spalling behaviour. It should be noted that the analysis does not consider buffer saturation, and therefore, there is no change in the thermal properties or mechanical properties during the course of the analysis. This is a conservative assumption both from a thermal and a mechanical viewpoint.

6.1.7 Optimized Layout

Based on the results from the preliminary near-field (infinite repository) optimization, two options are suitable for the multi-level repository layout. Using the same room to room spacing in both levels, a spacing of 36 m will meet the temperature criterion. The footprint of the multiple level repository would be 2 km × 1.45 km for both levels. Using the a different room to room spacing in each level, a spacing of 32 m in the upper level and a room to room spacing of 38 m in the lower level will meet the temperature criterion. The footprint of the multiple level repository would be 2 km × 1.5 km for the lower level and 2 km × 1.3 km for the upper level. Figure 6-12 shows the layout for the repository with 3.6 million used CANDU fuel bundles per level (same room to room spacing in both levels), including the underground demonstration facility in the upper repository. The size of the drifts and placement rooms remains unchanged from the single repository layout, as well as the radii of the approaches to the rooms from the perimeter drifts and cross cuts.

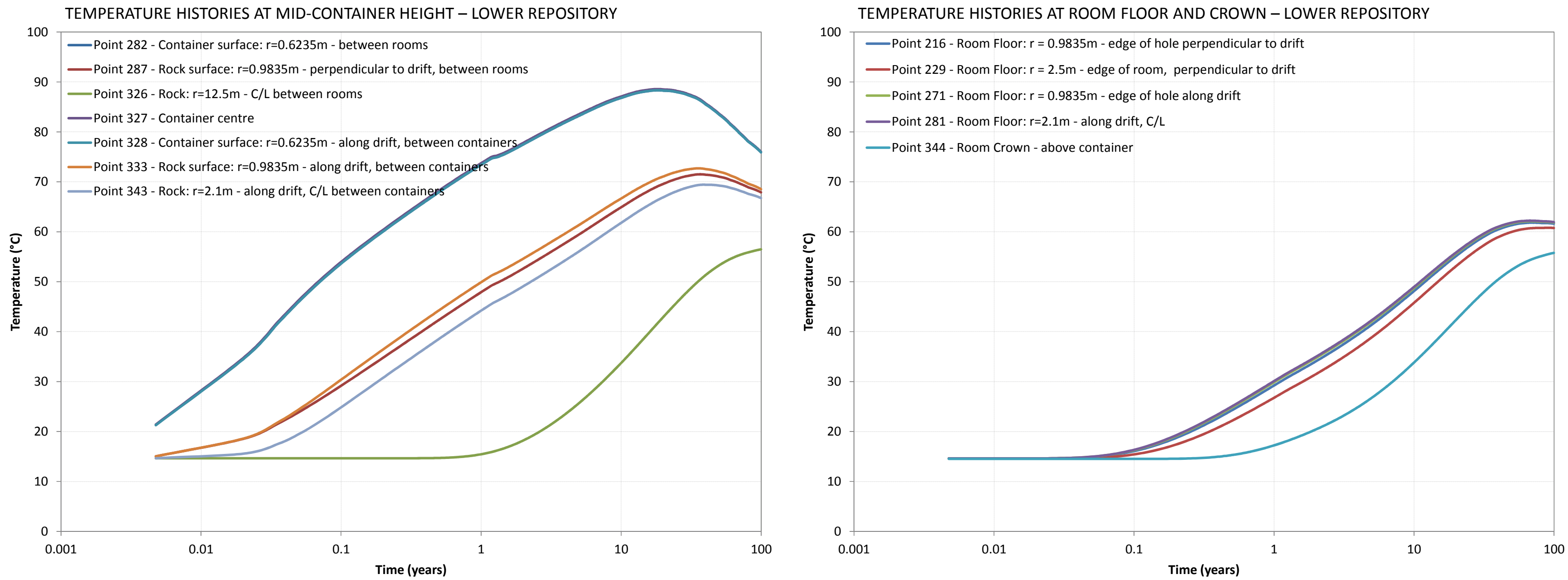

Figure 6-7: Temperature histories in the lower repository for a room spacing of 36 m

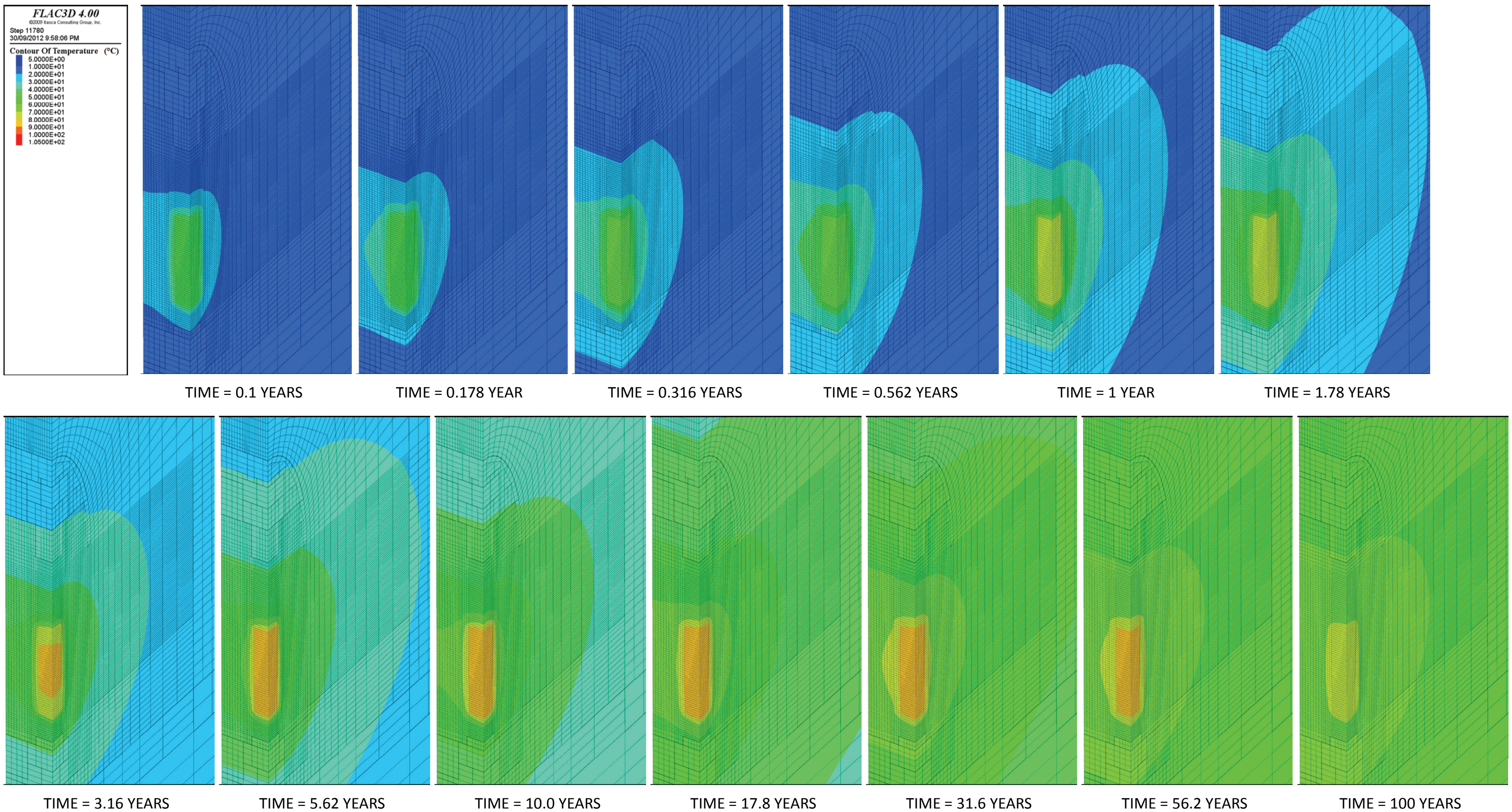

Figure 6-8: Temperature contours in ^{0}C at selected times (at each 1/4 log cycle of time).

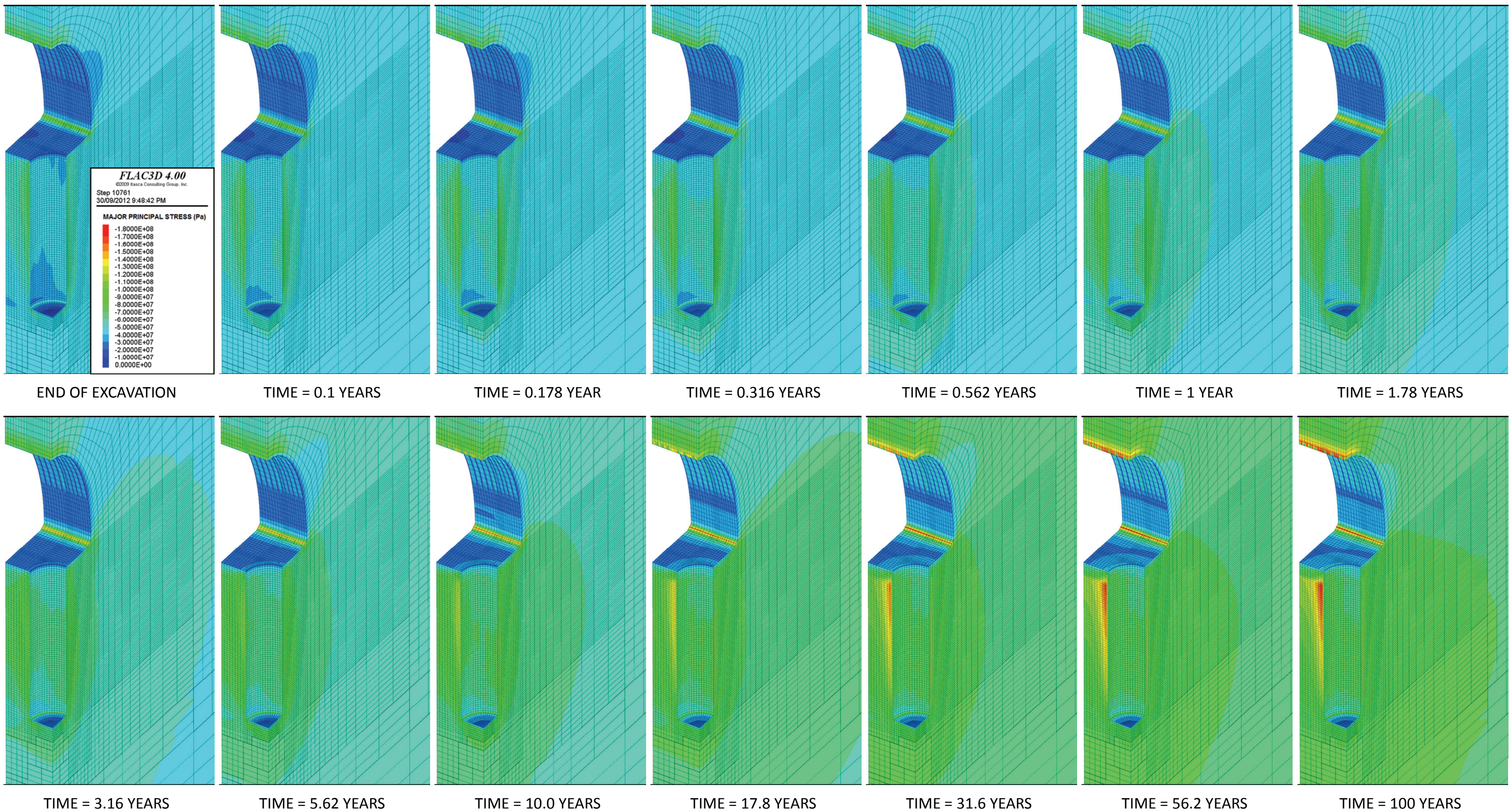

Figure 6-9: Major stress contours in Pa at selected times (at each 1/4 log cycle of time).

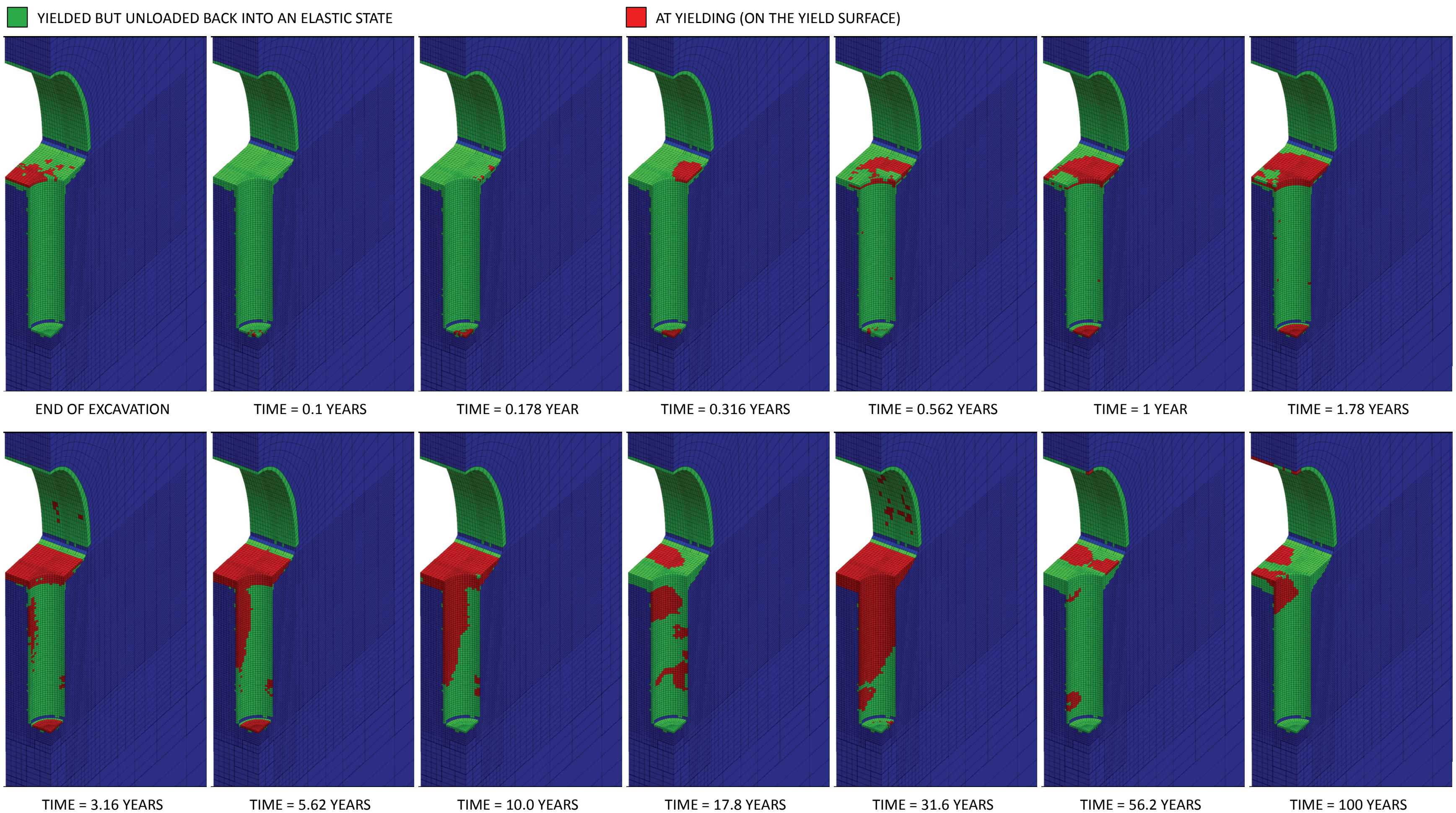

Figure 6-10: Damage zone evolution at selected times (at each 1/4 log cycle of time).

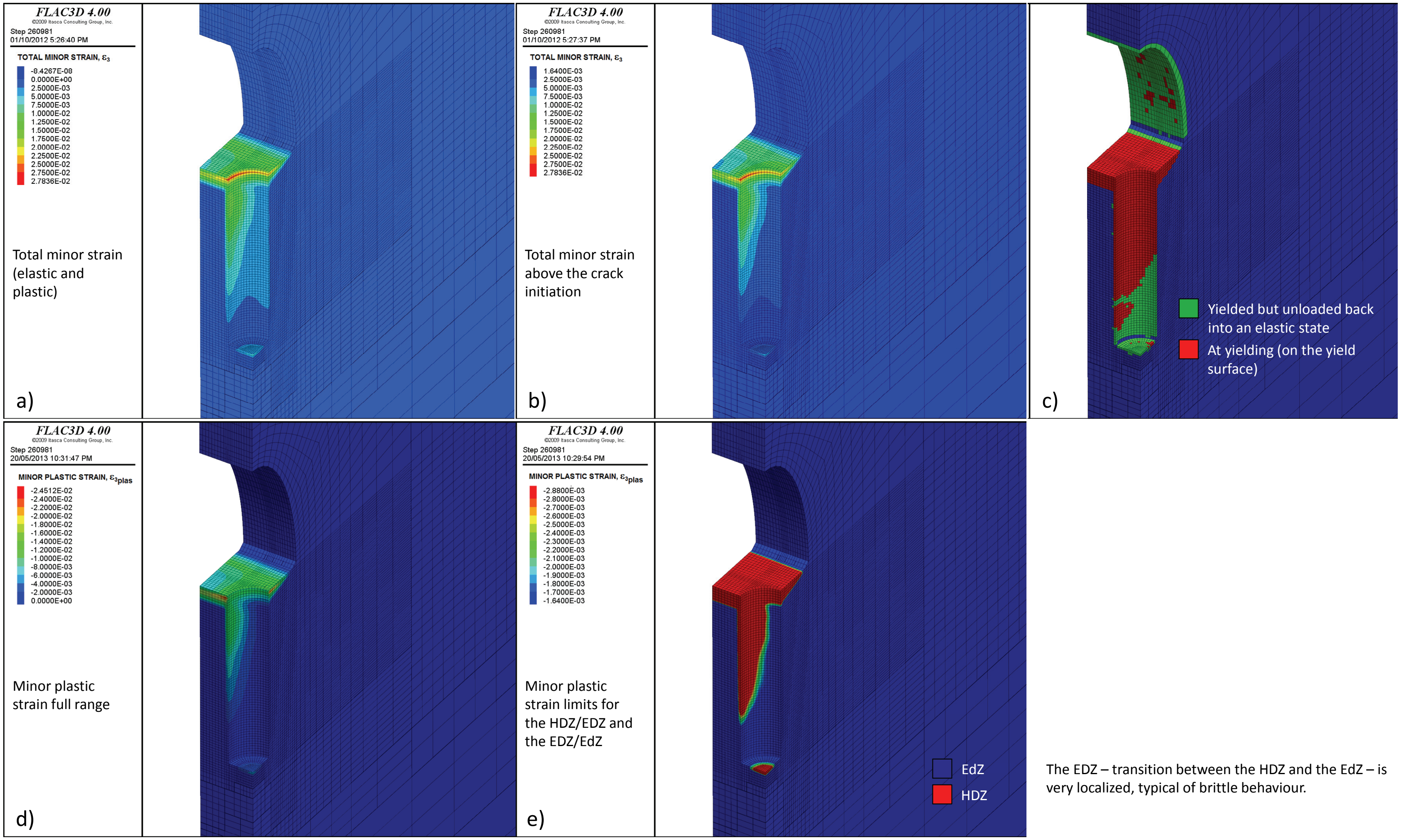

Figure 6-11: Delineation of the Damage Zones (HDZ, EDZ and EdZ).

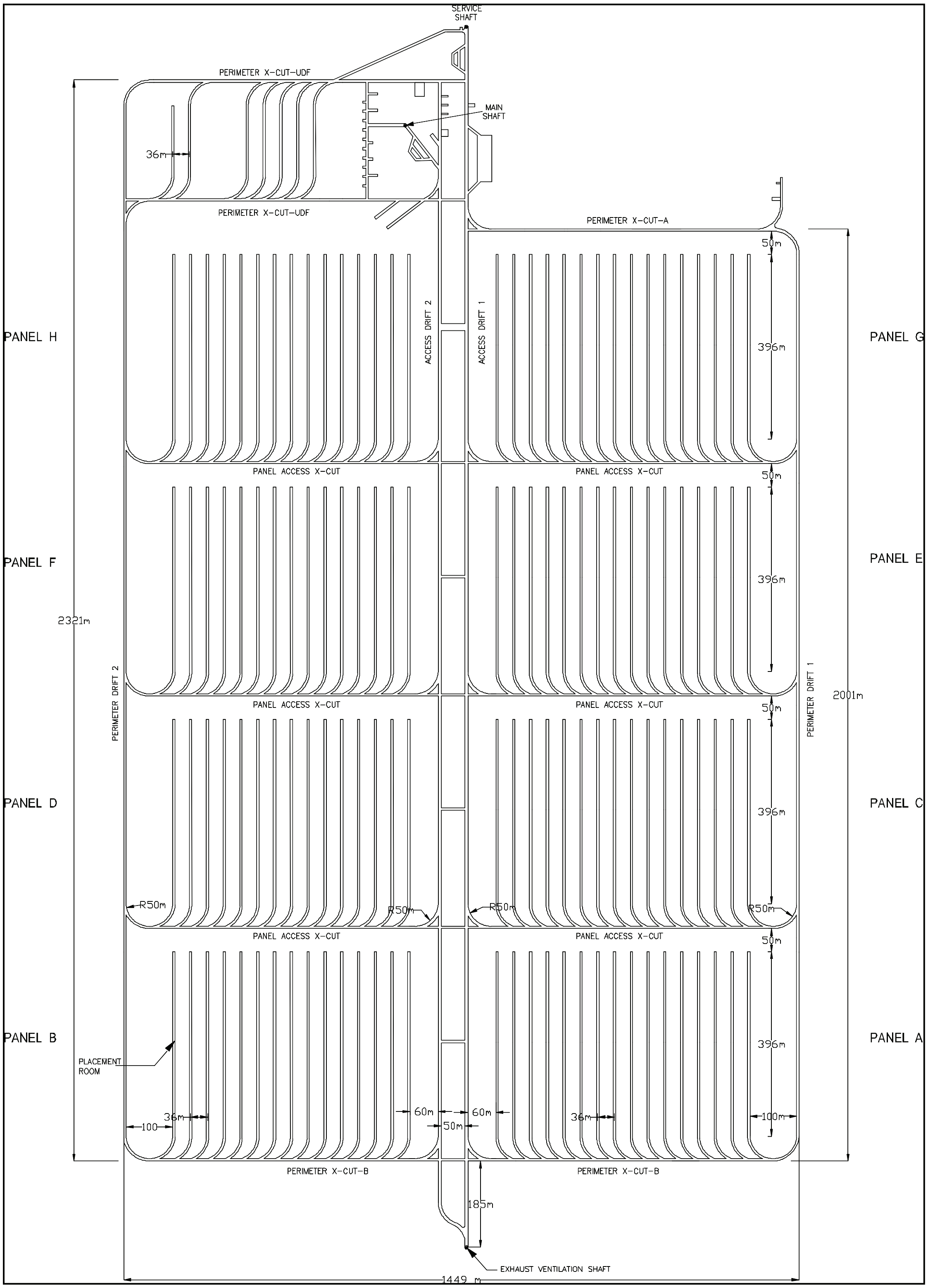

Figure 6-12: Optimized APM deep geological repository layout for 3.6 million used CANDU fuel bundles per level, including underground demonstration facility in the upper level.

6.2 Far-Field Modelling

Based on the results from the near-field optimization, the footprint of the multi-level repository is 2.0 km × 1.45 km. For the 7.2 million used CANDU fuel bundle, multi-level repository, one can take advantage of symmetry and only one quarter of the model needs to be discretized (see Figure 6-13). The lateral extent of the model boundaries was set at a distance of 2500 m from the edges of the repository footprint. The lower boundary was set at a depth of 2000 m. Figure 6-13 also shows the locations of the monitored points for comparison with the 'infinite' repository results.

6.2.1 Mechanical Boundary Conditions

6.2.1.1 7.2 million used CANDU fuel bundles (3.6 million bundles per level)

The boundary conditions of the quarter mesh set up for the 7.2 million used CANDU fuel bundle multi-level repository have to respect the two lines of symmetry, one at the x-axis, the other at the y-axis, where lateral movements in the direction normal to the boundaries are prevented. These two boundaries are allowed to move in the vertical direction. The top boundary of the model represents the ground surface and, as such, is allowed to deform in all directions. The other three boundaries (far-field) are set far away enough from the zone of influence such that the deformations should be negligible. Therefore, they can be either fixed in all three directions or just in the normal direction. The latter was chosen for the model in this report.

6.2.2 Thermal Boundary Conditions

6.2.2.1 3.6 million used CANDU fuel bundles

Similarly to the mechanical boundary conditions, the thermal conditions have to respect the two lines of symmetry, one at the x-axis, the other at the y-axis, where lateral heat flux in the direction normal to the boundaries is prevented. This is termed an adiabatic boundary condition. The top of the model, representing the ground surface has been set at a constant temperature of 5°C, while the bottom of the model (2000 m deep) has been set at a constant temperature of 29°C, based on a thermal gradient of 0.012°C/m. The two vertical far-field boundaries are also set at a constant temperature which varies linearly with depth, from 5°C at the top to 29°C at the bottom of the model.

The distance of the far boundaries of the model were established by using the analytical solution for an instantaneous rectangular heat source in a semi-infinite medium and plotting the temperature decay over time. Details of the solution can be found in Carvalho and Steed (2012).

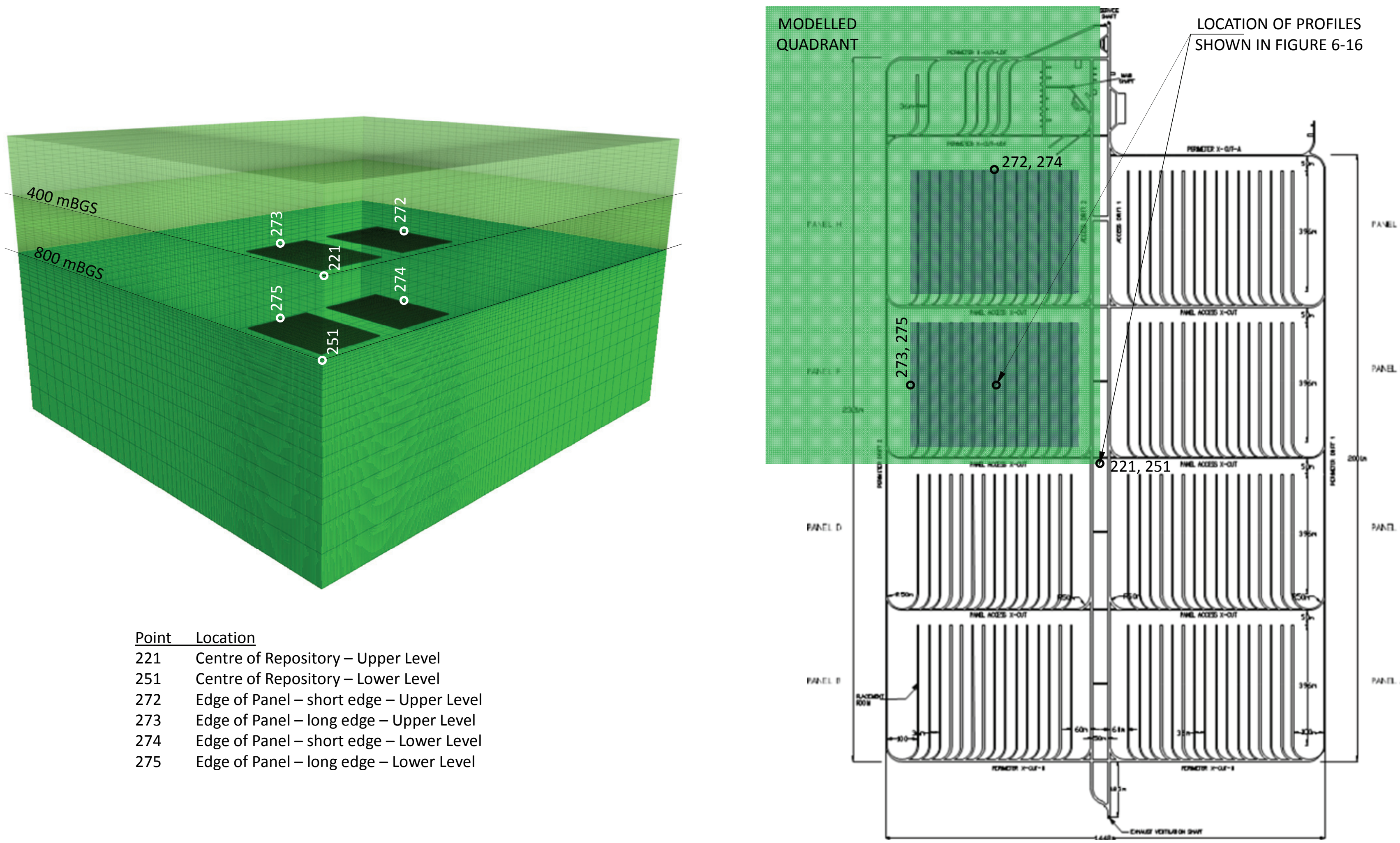

Figure 6-13: Finite difference mesh for the far-field model for 7.2 million bundles (3.6 million bundles in each level).

6.2.3 Heat Generation

The heat generation in the model is specified in W/m^3; therefore, a heat density generation should be calculated by dividing the heat output of each container by the tributary volume for one container (4.2 m × 36.0 m × 5 m). Heat generation was defined by the initial heat density, multiplied by a heat decay function (determined by normalizing the heat density generation, assuming 100% at 30 years out-of-reactor). This results in an initial heat density generation of 1.6775 W/m^3 at the time of placement (30 years out-of-reactor). The schedule for the IV-25 UFC heat output has been reported in Table 6-1 of Section 6.1.3.

6.2.4 Thermal Results

6.2.4.1 7.2 million used CANDU fuel bundles (3.6 million bundles per level)

The results from the far-field thermo-mechanical analysis are shown in Figures 6-14 and 6-15. The model has a cut-out section exposing both axis of the centre panel for a better view of the temperature distribution. The maximum temperature reached is just under 60°C in the lower repository and just over 50°C in the upper repository, at approximately 4000 and 2800 years after placement, respectively. The lower temperatures in the far field analyses can be explained by the following assumptions:

- the heat generation has been limited to the panel footprints;
- the pillars between panels were included in the analyses; and
- the repository is finite in extent.

6.2.4.1.1 Comparison with infinite repository

Results for the ‘infinite’ repository (with the same far-field mesh discretization) were reported in Section 6.1.4.4. This allows for comparison of the ‘infinite’ repository results with the ‘finite’ repository results to establish how much higher that second peak is in the case of the ‘infinite’ repository.

Figure 6-17 shows that the second temperature peak occurs at approximately 4000 and 2800 years after placement in lower and upper levels of the repository, respectively. In the centre of the repository, this second temperature peak is 40% lower in the finite repository than in the infinite one. It should be noted that the maximum temperature of the second peak at the edges of the repository is of the order of 10°C to 15°C cooler than that in the centre.

Figure 6-16 shows the temperature profiles at selected times for the infinite multi-level repository, the centre of a panel in the finite repository, and the centre of the finite repository (see Figure 6-13 for locations). The temperature profiles show a significant difference between the infinite repository and the finite repository. The difference between the temperature at the centre of a panel and the centre of the repository (which is in the centre pillars between panels) is 10°C to 15°C mainly due to the lack of sharp temperature peaks present in the heat generating cells.

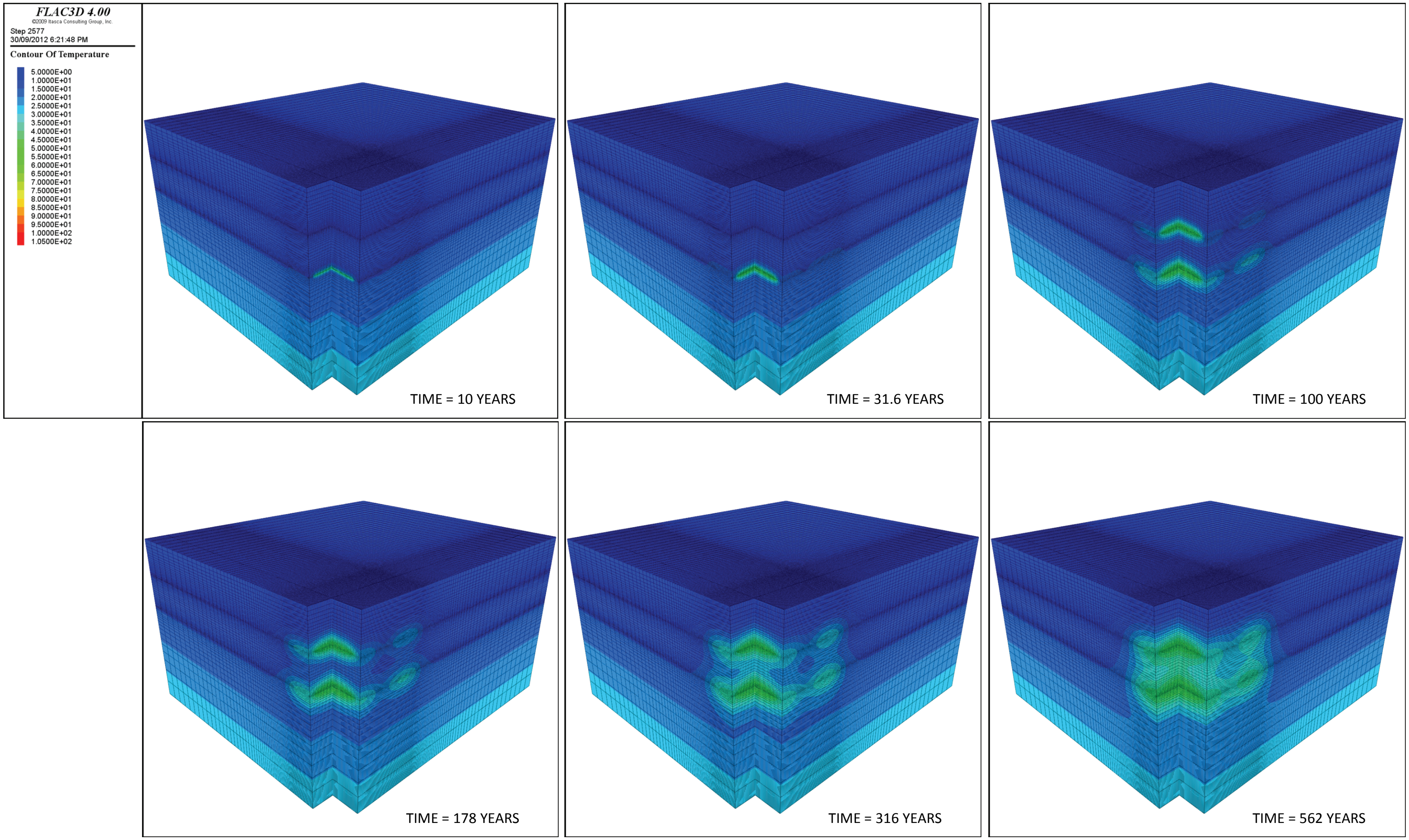

Figure 6-14: Temperature distribution with time in ^{0}C (10 years to 562 years) for the multi-level repository with 7.2 million used CANDU fuel bundles (3.6 million bundles in each level).

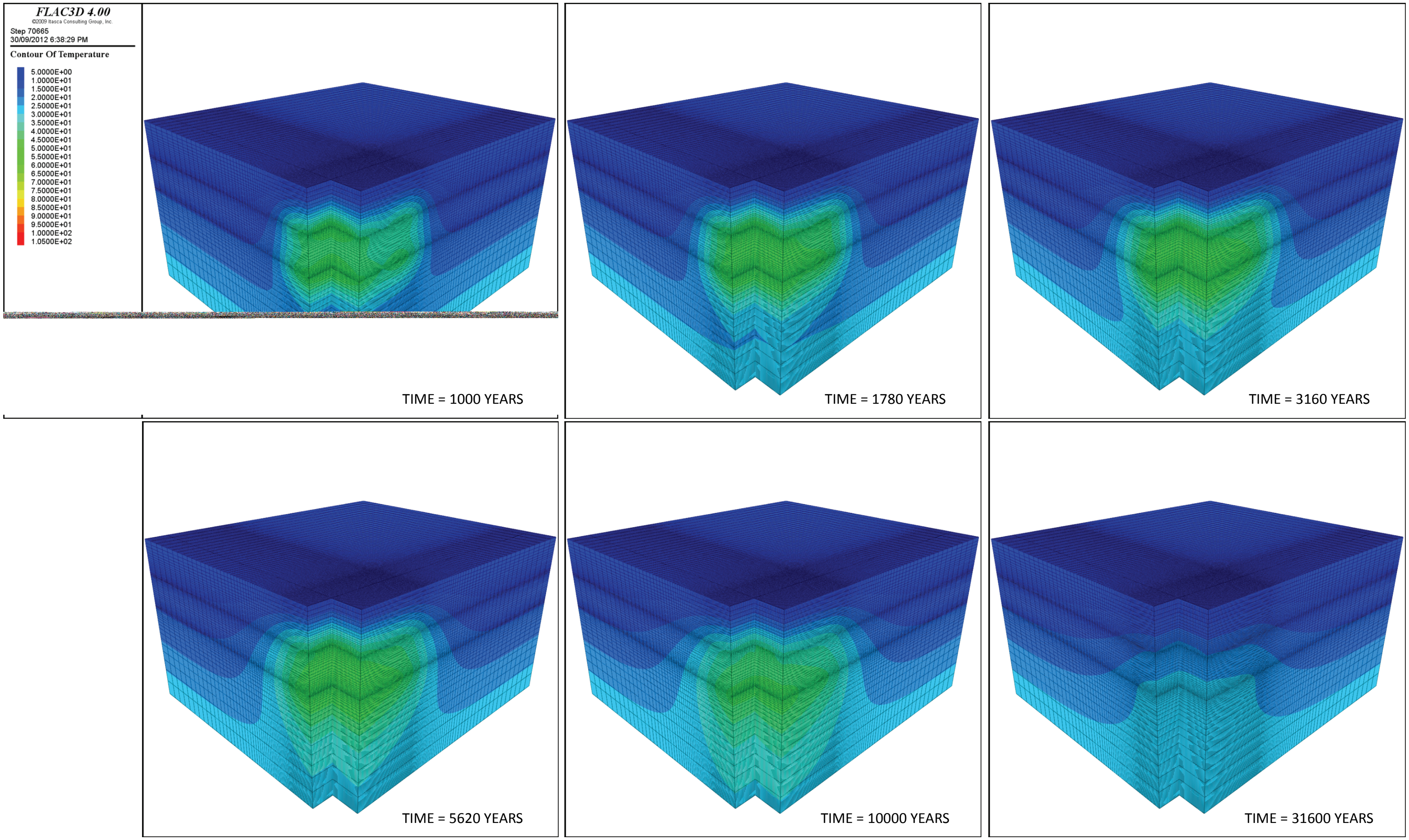

Figure 6-15: Temperature distribution with time in ^{0}C (1000 years to 31600 years) for the multi-level repository with 7.2 million used CANDU fuel bundles (3.6 million bundles in each level).

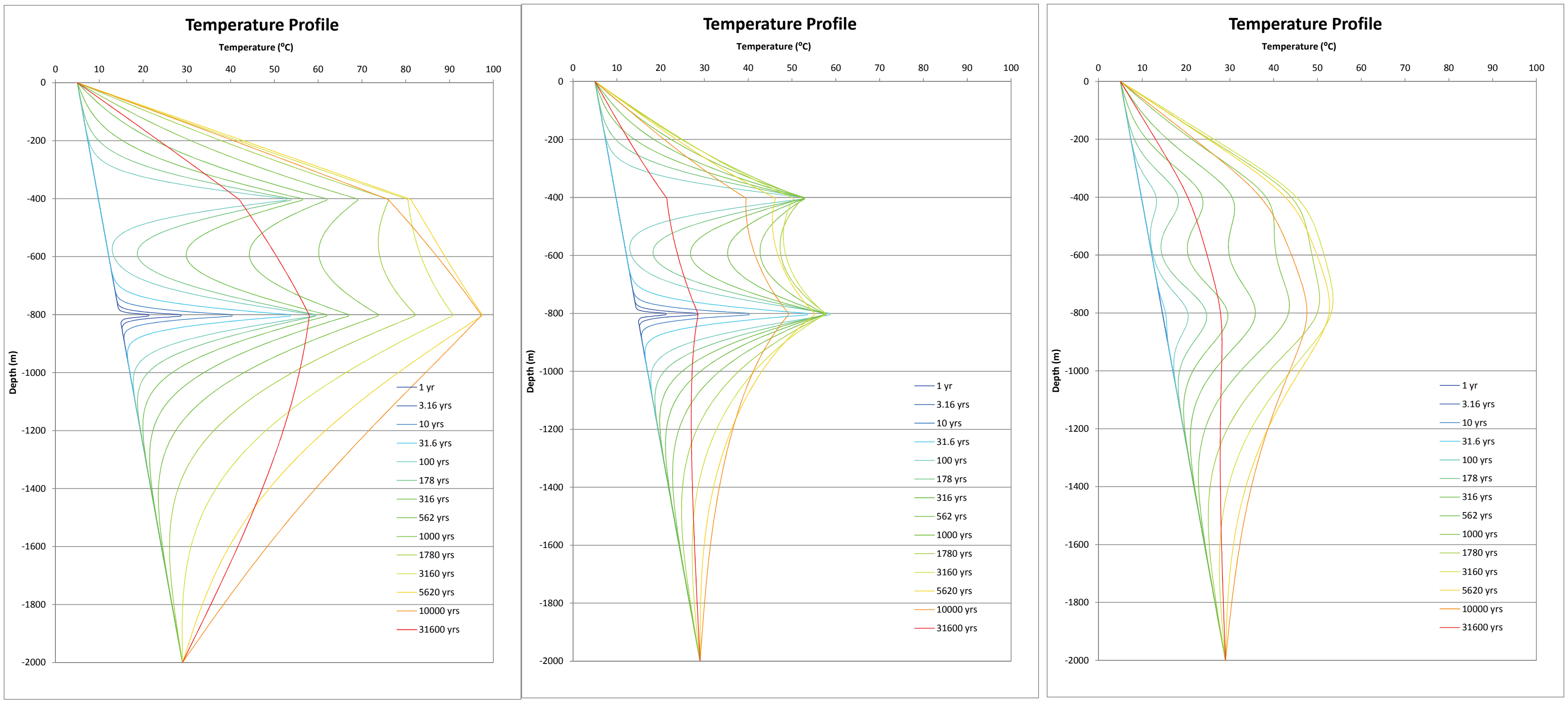

Multi Level – 7.2 million used CANDU fuel bundles – Infinite Repository

Multi Level – 7.2 million used CANDU fuel bundles – Finite Repository Centre of Panel

Multi Level – 7.2 million used CANDU fuel bundles – Finite Repository Centre of Repository

Figure 6-16: Temperature profiles at selected times for the multi-level repository with 7.2 million used CANDU fuel bundles (3.6 million bundles in each level).

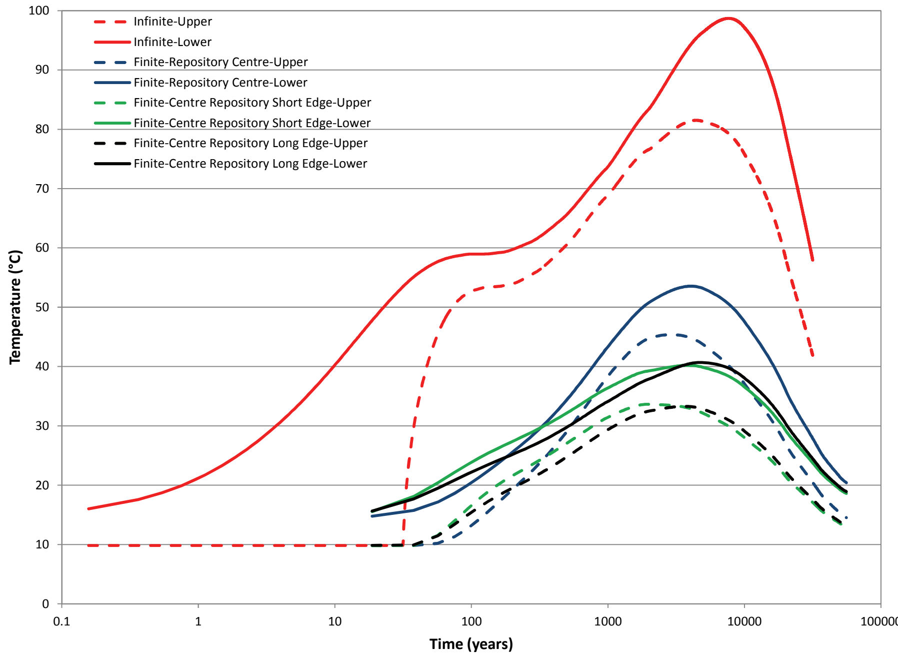

Figure 6-17: Comparison of the heat time histories between the finite and infinite repositories.

6.2.5 Uplift and Distressed Zone

6.2.5.1 7.2 million used CANDU fuel bundles (3.6 million bundles per level)

Results from the far-field thermo-mechanical analysis are shown in Figures 6-18 through 6-21. Figures 6-18 and 6-19 show the evolution of the uplift as the repository heats up, resulting in a maximum uplift of 40 cm above the centre of the repository at approximately 5000 years after placement of the containers. The uplift can be felt up to a distance of about 1600 m from the repository edges (about 2.5 cm at that distance).

Figure 6-20 shows contours of the minor principal stress and Figure 6-21 shows the extent of the tensile zone at surface. Tension is only felt at surface 300 years after placement and the tension zone grows to approximately the size of the footprint of the repository along the long axis and to almost double the repository width along the short axis. The tensile zone is felt to a maximum depth of about 90 m at the centre of the repository by 5000 years after placement. The tensile zone disappears after the repository has cooled down at about 20,000 years.

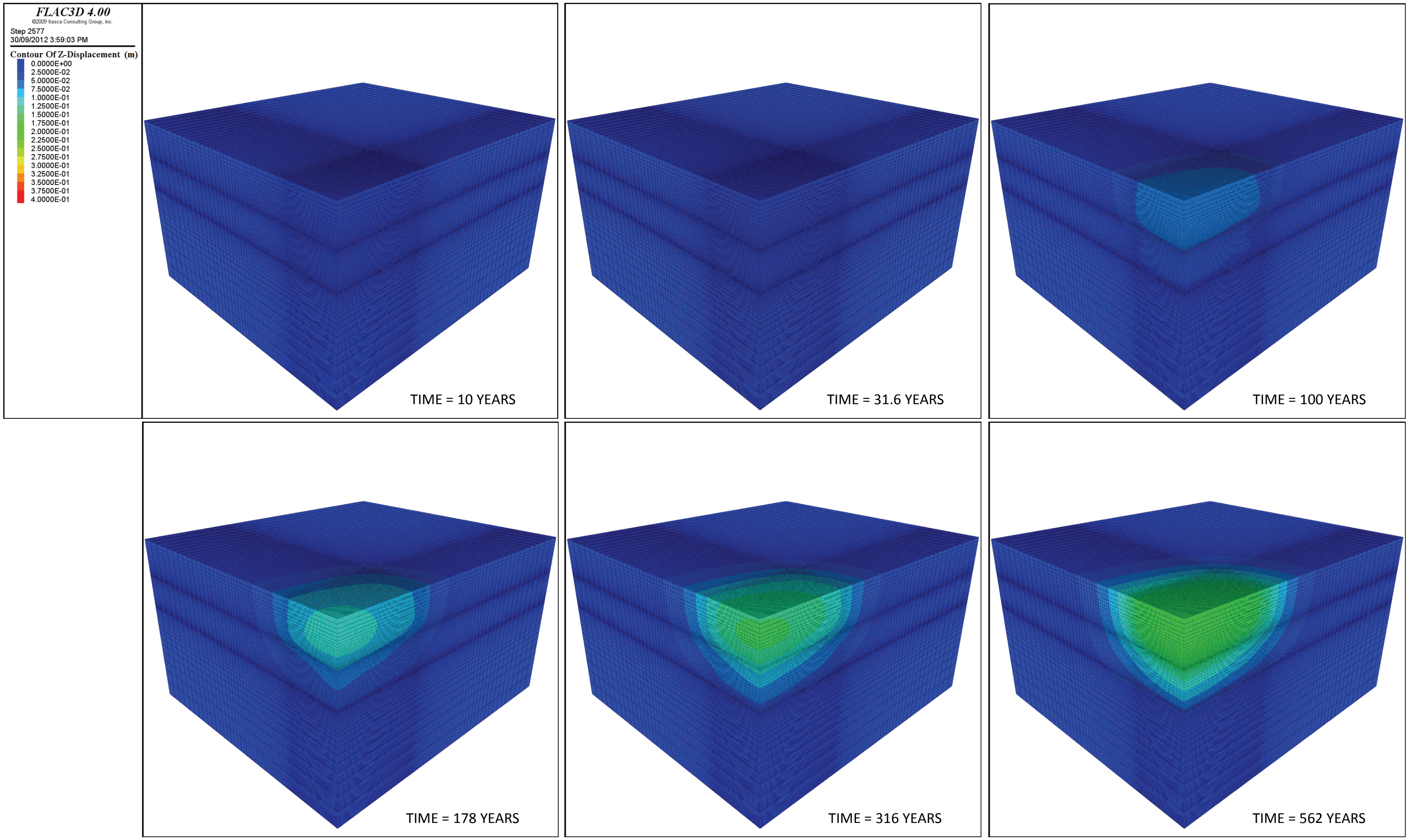

Figure 6-18: Vertical displacement distribution with time in metres (10 years to 562 years) for the multi-level repository with 7.2 million used CANDU fuel bundles (3.6 million bundles in each level).

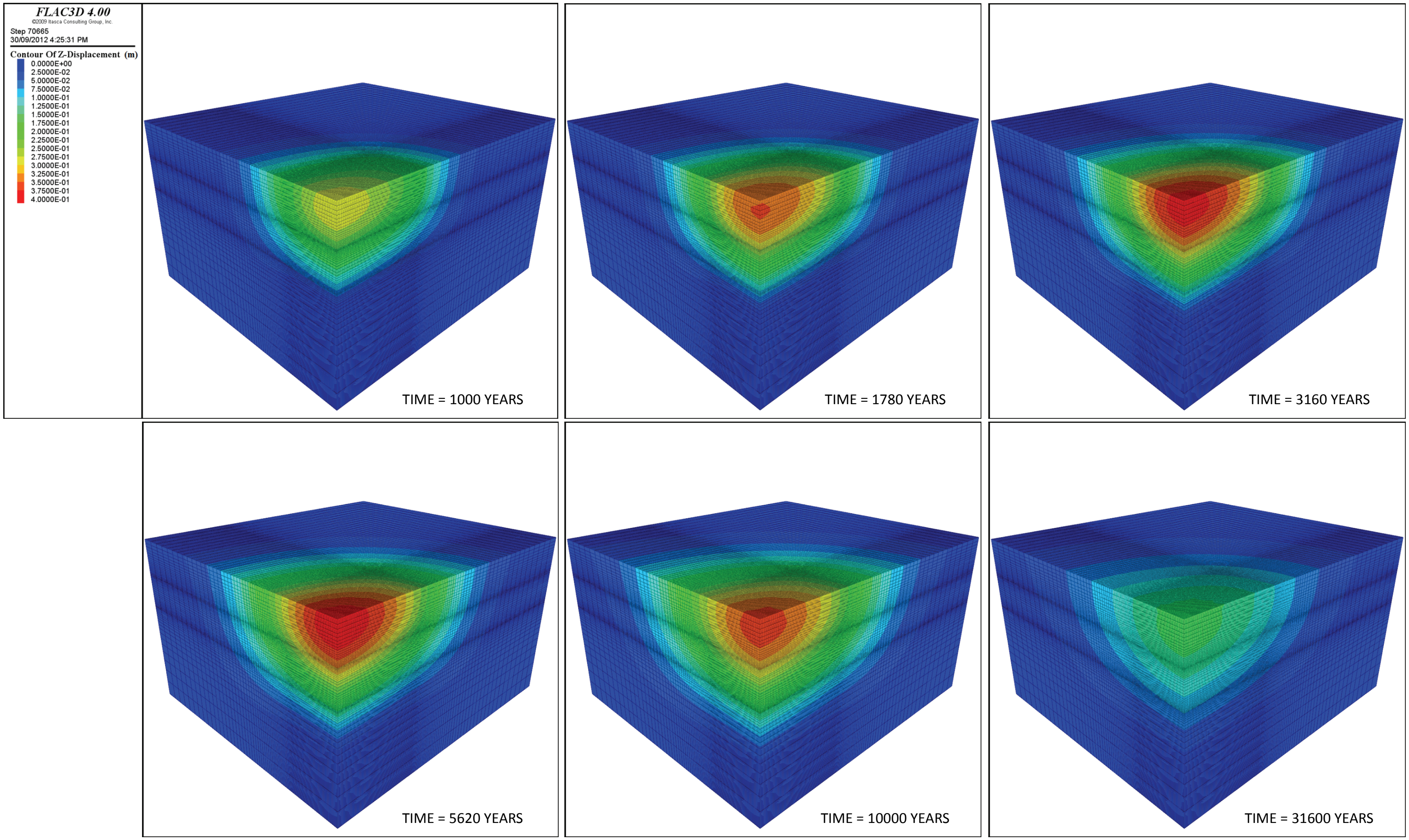

Figure 6-19: Vertical displacement distribution with time in metres (1000 years to 31600 years) for the multi-level repository with 7.2 million used CANDU fuel bundles (3.6 million bundles in each level).

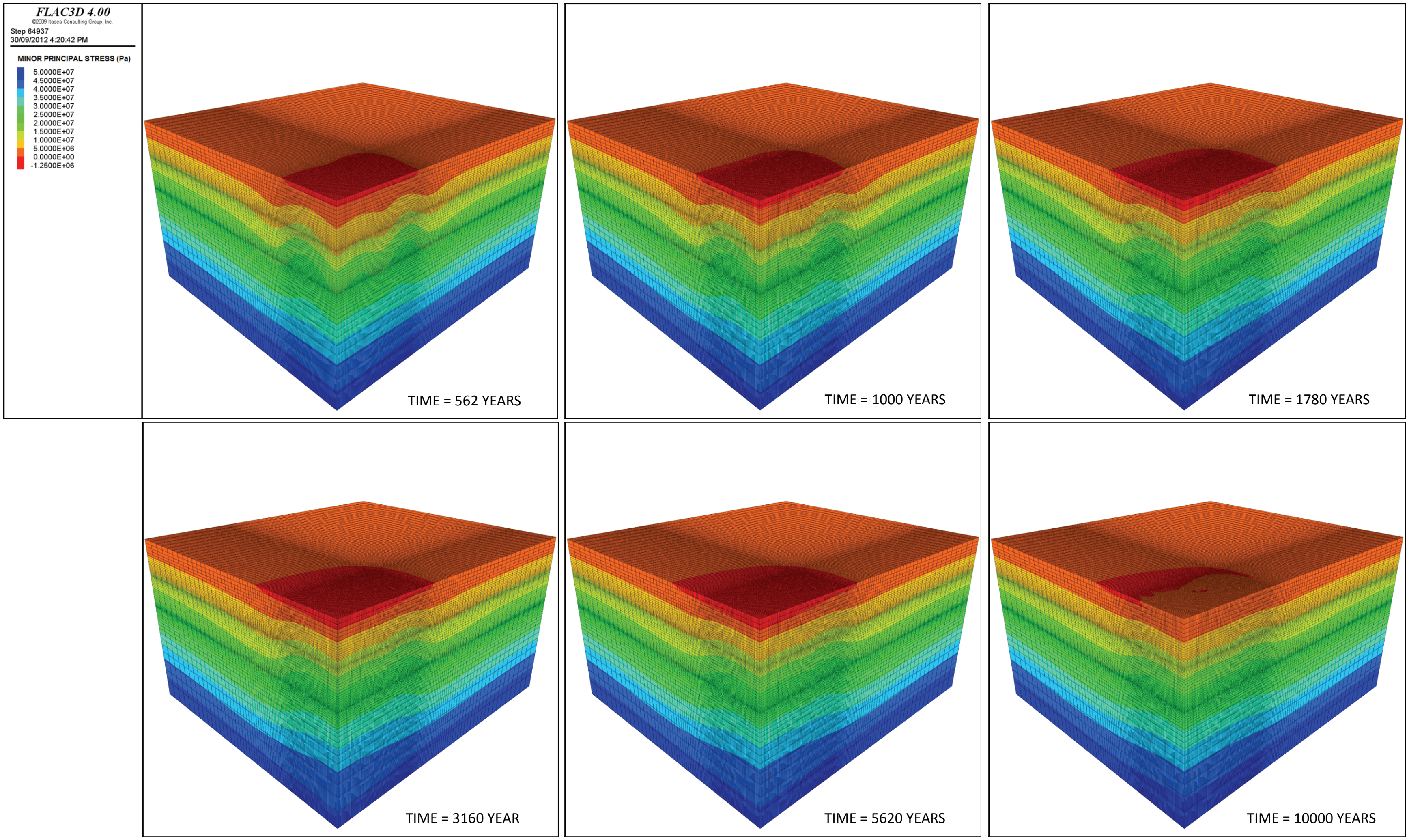

Figure 6-20: Minor principal stress distribution with time in Pa (562 years to 10000 years) for the multi-level repository with 7.2 million used CANDU fuel bundles (3.6 million bundles in each level).

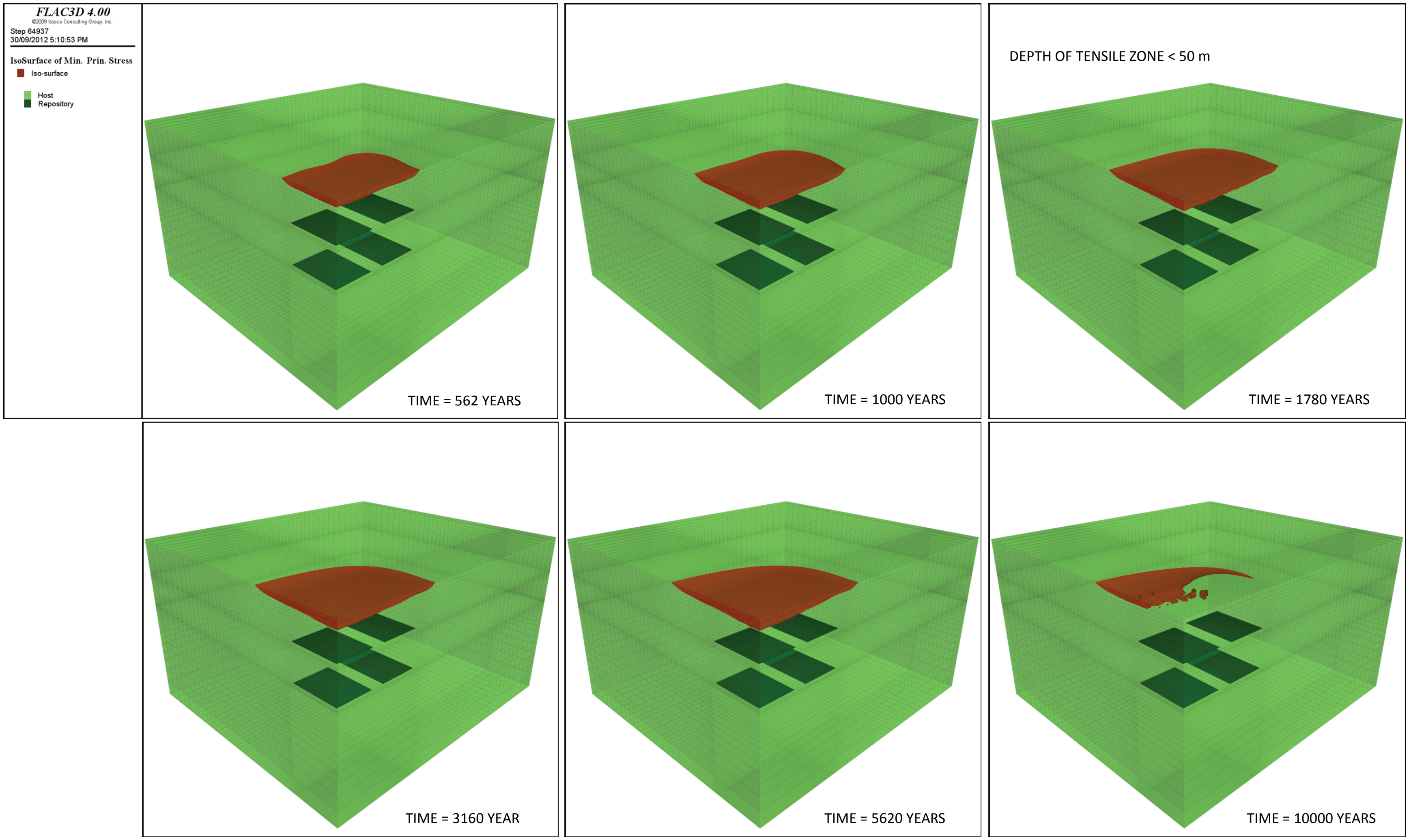

Figure 6-21: Tensile zone with time (562 years to 10000 years) for the multi-level repository with 7.2 million used CANDU fuel bundles (3.6 million bundles in each level).

7. CONCLUSIONS

Thermo-mechanical analyses were undertaken for the reference APM repository based on an alternate case inventory of 7.2 million used CANDU fuel bundles placed in two levels in order to optimize the underground footprint of the repository. The analyses also address the mechanical and thermally induced stress regimes and damage zones around the placement rooms and in-floor boreholes for the multi-level repository. In addition to the impact of the containers on the in-floor boreholes and placement rooms (near field), the report addresses the thermally induced uplift at surface as well as any thermally induced distressed zone at surface (far-field) for both the alternate inventory of 7.2 million used CANDU fuel bundles placed in two levels.

Through thermo-mechanical analysis of a unit cell of the repository (centreline to centreline of placement rooms, and centreline to centreline of containers), it has been established that, with the repository levels at a depth of 400 m and 800 m and a fixed distance of 4.2 m between containers, the placement rooms can be spaced at 36 m centreline to centreline in both levels without the peak temperature of the containers exceeding 100°C. Alternatively, the placement rooms can be spaced at 32 m centreline to centreline in the upper level and 38 m centreline to centreline in the lower level without the peak temperature of the containers exceeding 100°C.

Far-field analysis of the repository for the alternate inventory (7.2 million used CANDU fuel bundles) placed in two levels showed that the uplift over the centre of the repository is of the order of 40 cm and that the extent of the tensile zone is of about the same size as the footprint of the repository along the long and about double the width of the repository. The depth of the tensile zone at the time of its maximum extent (about 5000 years after placement) is of the order of 90 m.

REFERENCES

Barton, N.R., R. Lien, and J. Lunde, 1974. Engineering classification of rock masses for the design of tunnel support. Rock Mech. 6(4), 189-239.

Baumgartner, P. 2005. Scoping analyses for the design of a deep geologic repository in sedimentary rock. Ontario Power Generation Nuclear Waste Management Division Report No. 06819-REP-01300-10093-R00. Toronto Canada

Baumgartner, P. 2006. Generic Thermal-Mechanical-Hydraulic (THM) Data for Sealing Materials. Volume 1: Soil-water Relationships. Ontario Power Generation Nuclear Waste Management Division Report No. 06819-REP-01300-10122, Toronto, Ontario.

Bieniawski, Z.T. 1976. Rock mass classification in rock engineering. In Exploration for rock engineering, proc. of the symp., (ed. Z.T. Bieniawski) 1, 97-106. Johannesburg: Balkema.

Carslaw, H.S. and J.C. Jaeger, Conduction of heat in solids, 2nd edition. Oxford University Press, London, 1959.

Carvalho, J.L., and C.M. Steed. 2012. Thermo-mechanical analysis of a single level repository for used nuclear fuel. Prepared by Golder Associates Ltd. Nuclear Waste Management Organization Report APM-REP-00440-0010. Toronto, Canada.

Garisto, F., A. D'Andrea, P. Gierszewski and T. Melnyk. 2004. Third Case Study – Reference Data and Codes. Ontario Power Generation Nuclear Waste Management Division Report No. 06819-REP-01200-10107-R00, Toronto, Ontario.

Gierszewski, P., M. Jensen, P. Maak and A. Vorauer. 2004. Third Case Study Site and Design Description. Ontario Power Generation Report No. 06819-REP-01200-10124, Toronto, Ontario.

Hoek, E., C. Carranza-Torres and B.T. Corkum, Hoek-Brown Failure Criterion – 2002 Edition. Proc. of the 5th North American Rock Mechanics Symposium and the 17th Tunnelling Association of Canada Conference: NARMS-TAC 2002. July 7-10, 2002, Toronto, Ontario, Canada, pp. 267-273.

Kaiser, P.K. and S. Maloney. 2005. Review of the Ground Stress Database for the Canadian Shield. Prepared by MIRARCO Mining Innovation. Ontario Power Generation Nuclear Waste Management Division Supporting Technical Report No. 06819-REP-01300-10107-R00, Toronto, Ontario.

NRCan. 2007. Governor General in Council decision selecting Adaptive Phased Management as Canada's approach for the long-term management of nuclear fuel waste, pursuant to section 15 of the Nuclear Fuel Waste Act. Privy Council File: P.C. 2007-834, dated May 31, 2007.

NWMO. 2005. Choosing a Way Forward: The Future Management of Canada's Used Nuclear Fuel – Final Study. Nuclear Waste Management Organization.

SNC-Lavalin Nuclear Inc. 2011. APM Conceptual Design and Cost Estimate Update – Deep Geological Repository Design Report – Crystalline Rock Environment – Copper Used Fuel Container. Prepared by SNC-Lavalin Nuclear Inc. for the Nuclear Waste Management Organization. APM-REP-00440-0001.

Srivastava, R.M. 2002. Probabilistic Discrete Fracture Network Models for the Whiteshell Research Area. Prepared by FSS Canada Consultants Inc. Ontario Power Generation. Report No. 06819-REP-01200-10071-R00, Toronto, Ontario.